Blood cultures contain populations of genetically diverse *Candida albicans* strains that may differ in echinocandin tolerance and virulence

Giuseppe Fleres,[1] Shaoji Cheng,[1] Hassan Badrane,[1] Christopher L. Dupont,[2] Josh L. Espinoza,[2] Darren Abbey,[3] Eileen Driscoll,[1] Anthony Newbrough,[1] Binghua Hao,[1] Akila Mansour,[4] *M. Hong Nguyen,[1,4 #] *Cornelius J. Clancy[1,5]

[1]University of Pittsburgh, Pittsburgh, PA, USA
[2]J. Craig Venter Institute, La Jolla, CA, USA
[3]University of Minnesota, Minneapolis, MN, USA
[4]University of Pittsburgh Medical Center, Pittsburgh, PA, USA
[5]VA Pittsburgh Healthcare System, Pittsburgh, PA, USA

*These authors contributed equally: M. Hong Nguyen, Cornelius J. Clancy. The order in which they are listed is based on mutual consent

Running title: *C. albicans* diversity in blood cultures

[#]Corresponding author:
M. Hong Nguyen, M.D.
University of Pittsburgh
Biomedical Science Tower, Starzl Institute
200 Lothrop Street, E-1052
Pittsburgh, PA 15203
Email: MHN5@pitt.edu
Phone: 412-383-5193

Abstract: 250 words

Text: 3,478 words

Abstract.

It is unknown whether within-patient *Candida albicans* diversity is common during bloodstream infections (BSIs). We determined whole genome sequences of 10 *C. albicans* strains from blood cultures (BCs) in each of 4 patients. BCs in 3 patients contained mixed populations of strains that differed by large-scale genetic variants, including chromosome (Chr) 5 or 7 aneuploidy (*n*=2) and Chr1 loss of heterozygosity (*n*=1). Chr7 trisomy (Tri7) strains from patient MN were attenuated for hyphal and biofilm formation in vitro compared to euploid strains, due at least in part to *NRG1* over-expression. Nevertheless, representative Tri7 strain M1 underwent filamentation during disseminated candidiasis (DC) in mice. M1 was more fit than euploid strain M2 during DC and mouse gastrointestinal colonization, and in blood ex vivo. M1 and M2 exhibited identical echinocandin minimum inhibitory concentrations, but M2 was more tolerant to micafungin in vitro. Furthermore, M2 was more competitive with M1 in mouse kidneys following micafungin treatment than it was in absence of micafungin. Tri7 strains represented 74% of patient MN's baseline BC population, but after 1d and 3d of echinocandin treatment, euploid strains were 93% and 98% of the BC population, respectively. Findings suggest that echinocandin tolerant, euploid strains were a subpopulation to more virulent Tri7 strains at baseline and then were selected upon echinocandin exposure. In conclusion, BCs in at least some patients are comprised of diverse *C. albicans* populations not recognized by the clinical lab, rather than single strains. Clinical relevance of *C. albicans* diversity and antifungal tolerance merits further investigation.

Keywords: *Candida albicans*; Bloodstream infections; Genetic diversity; Echinocandin tolerance; Aneuploidy; Chromosome 7 trisomy

Introduction.

Clinical strains of *Candida* spp. from sites of mucosal colonization and longitudinal *Candida* strains from sites of invasive disease often demonstrate within-host genetic and phenotypic diversity.[1,2,3-6 4,5,7] The long-standing paradigm is that most fungal or bacterial sterile site infections reflect proliferation of a single, genetically identical strain that passes through a bottleneck ("single organism" hypothesis).[8-10] In recent studies, however, we and others have shown that blood cultures (BCs) from patients with *Staphylococcus aureus*, carbapenem-resistant *Klebsiella pneumoniae* (CRKP) or *Candida glabrata* bloodstream infections (BSIs) can be comprised of genetically and phenotypically diverse strains, including strains unrecognized by the clinical laboratory that differ in antimicrobial susceptibility.[11-13] Within-patient *C. glabrata* strains differed by single nucleotide polymorphisms (SNPs) and, to a lesser extent, insertions-deletions (indels), gene copy number variations, presence/absence of specific genes and chromosomal rearrangements.

C. albicans is the most intrinsically virulent *Candida* sp. and the leading cause of candidemia globally.[14] *C. albicans* differs from *C. glabrata* in having a diploid, rather than haploid genome. In this study, we determined whether contemporaneous *C. albicans* strains from positive BCs of patients with BSIs were genetically and phenotypically distinct, and we compared diversity of strains from longitudinal BCs of patients with persistent BSIs.

Results.

Genetic diversity of *C. albicans* strains. We performed whole genome sequencing (WGSing; Illumina NextSeq) on 10 strains from individual colonies in each of 4 patients [Supplemental Table 1]. For patient G, 10 strains were sequenced from the baseline (day (d)-0) BC, including the index strain from the clinical laboratory and a strain from each of 9 randomly-selected colonies. For other patients, index and 4 randomly-selected strains were sequenced from both baseline and last positive BCs (collected 3d (patient AB), 12 d (QR) and 13 d (MN) after

baseline). Strains had 8 pairs of chromosomes and 14.24-14.82 Mbp genomes. On average, 98% of reads aligned to the reference *C. albicans* SC5314 genome (range: 96%-99%). Strains clustered by patient upon SNP phylogenetic analysis [Figure 1]. Within-patient strains differed by 0-7 (AB), 7-42 (G), 3-36 (MN) and 8-28 (QR) SNPs [Supplemental Table 2]. Within 3 patients, strains also differed by 1-8 (G), 0-9 (MN) and 1-6 (QR) indels.

Large-scale, within-patient genetic differences among strains were observed in 3 of 4 patients (G, MN, QR) [Figure 2. Within 2 patients (G, MN), strains differed by whole chromosome aneuploidies. In patient G, index strain G1 exhibited trisomy of chromosome (Chr) 5 (Tri5); other strains were euploid [Figure 2A]. In patient MN, 4 of 5 strains from the baseline BC (index strain M1, M3-M5) exhibited trisomy of Chr7 (Tri7); 1 of 5 strains from baseline (M2) and all 5 strains from d13 BCs (index strain N1, N2-N5) were euploid [Figure 2B]. Ploidy was confirmed by quantitative real-time PCR (qPCR) [Supplemental Table 3; Supplemental Figure 1].[12,15] In patient QR, loss of heterozygosity (LOH) of Chr1 was detected in 7 of 10 strains, including 2 of 5 baseline (index strain Q1 and Q2) and all 5 d12 (index strain R1, R2-R5) strains [Figure 2C]. R1-R5 also had segmental LOH of Chr7, which was not present in Q1-Q5. Within-patient AB strains did not show large-scale genetic variations.

Screening phenotypes of *C. albicans* strains. All 40 strains were susceptible to echinocandins and azoles. Within-patient minimum inhibitory concentrations (MICs) were within 2-fold. Strains from patients AB and QR formed normal hyphae in liquid media (YPD with 10% fetal bovine serum, RPMI1640 with 2% glucose, Spider; 37°C) and on solid agar (RPMI1640 with 2% glucose, Spider, M199; 30°C). Strains from patient G were impaired in hyphal formation in liquid media and on solid agar [Supplemental Figure 2]. Strains from patient MN formed normal hyphae in liquid media. On solid agar, however, all 4 Tri7 strains (baseline strains M1, M3-M5) were impaired in hyphal formation, whereas all 6 euploid strains (baseline M2 and d13

N1-N5) formed robust hyphae [Figure 3]. Tri7 strains also produced <30% of biofilm that was generated by euploid strains, as measured by crystal violet assay [Figure 4; *p*-values< 0.0001].

Phenotypic diversity of *C. albicans* strains from patient MN. We chose strains from patient MN for more in-depth phenotypic assays because they demonstrated genetic differences that correlated with differences in hyphal and biofilm formation, and serial positive BCs over 13d were available for study. The timeline of *C. albicans*-positive BCs and antifungal treatment is shown in Supplemental Figure 3.

Micafungin responsiveness. We first tested serial ten-fold dilutions of each strain for responsiveness to micafungin and other stress-inducing agents in dot-blot assays. Tri7 strains (M1, M3, M4, M5) were more susceptible to Congo red (200 µg/mL), sodium dodecyl sulfate (0.04%) and micafungin (0.03 µg/mL) at 30ºC and 39ºC than were euploid strains [Figure 5A]. There were no significant differences among strains in presence of fluconazole (1 µg/mL), methyl methane sulfonate (0.02%), hydrogen peroxide (H_2O_2, 2.5mM), sodium chloride (1M) or caffeine (10 mg/mL).

We next evaluated MN strains for micafungin tolerance (enhanced growth in presence of drug compared to control, without changes in MIC) using disk diffusion (fraction of growth (FoG)) and liquid microdilution (supra-MIC growth (SMG)) assays.[16,17] FoG of euploid strains within zones of 80%, 50% and 20% inhibition by micafungin (FoG_{80}, FoG_{50}, FoG_{20}) were higher than those of Tri7 strains (*p*=0.05, 0.03 and 0.008, respectively) [Figure 5B]. Likewise, mean SMG (average growth within micafungin-containing wells above MIC_{50}/growth in absence of micafungin) of euploid strains was higher than that of Tri7 strains (*p*=0.0003) [Figure 5C]. Therefore, euploid strains were more tolerant than Tri7 strains to micafungin by both FoG and SMG.

NRG1 dose effect. Decreased filamentation of some *C. albicans* Tri7 strains has been linked to dose-dependent expression of Chr7 gene *NRG1*, which encodes a negative regulator of certain hyphal genes.[15] We demonstrated by qRT-PCR that *NRG1* expression by Tri7 strain M1 was ~1.5 fold higher than that by euploid strains [Supplemental Figure 4A]. [18] We created *NRG1* over-expression strains in euploid M2 and N1 backgrounds (strains M2-Nrg1OE and N1-Nrg1OE, respectively). *NRG1* expression by M2-Nrg1OE and N1-Nrg1OE was ~1.8-fold and ~1.6-fold higher than by the respective euploid parent strains (p=0.001) [Supplemental Figure 4A]. Over-expression strains had reduced hyphal and biofilm formation compared to euploid parent strains (biofilm p-values <0.0001) [Supplemental Table 3; Supplemental Figures 4B-C].

Competitive growth in vitro and in blood ex vivo. Since Tri7 and euploid strains comprised a mixed population within patient MN's baseline BC, we studied competitive fitness of bar-coded Tri7 strain M1 and bar-coded euploid strain M2 under various conditions. Bar-coded strains did not differ from respective parent strains during growth in YPD media or by echinocandin MICs or in hyphal and biofilm formation.

We conducted competitive growth assays (1:1 ratio, $1x10^4$ colony forming units (CFUs)/mL each) in liquid YPD media at 39°C in presence or absence of H_2O_2 (1 mM) or micafungin (0.125 µg/mL).[15] There were no significant differences in competitive fitness between strains over 3, 6 or 9d in YPD alone or in presence of H_2O_2, as determined by bar code sequencing [Figure 6A]. Strain M2 was more fit than M1 at each time point in the presence of micafungin (p <0.0001), consistent with FoG and SMG tolerance data. During ex vivo competitive assays in fresh blood from a healthy volunteer at 37°C ($1x10^4$ CFUs)/mL each), M1 was significantly more fit than M2 over 1, 3 and 7d [Figure 6B].

Competitive mouse models of GI colonization and disseminated candidiasis (DC).[15] We co-infected male and female mice with bar-coded M1 and M2 ($1x10^8$ CFUs each) by gavage. M1 significantly out-competed M2 within stool on d1, d3 and d7 [Figure 7A], and in ileum

and colon on d7 [Figure 7B]. We then co-infected mice via lateral tail vein with bar-coded strains ($5x10^5$ CFUs each). M1 significantly out competed M2 within kidneys, the major DC target organ, at d1, 3 and 7 [Figure 7C]. We also treated a group of M1:M2 co-infected mice with a single dose of micafungin (8.3 mg/kg/mouse intraperitoneal, 30 minutes post-infection). Strain M2 was 59% more competitive with M1 in kidneys at 24h following treatment than it was in absence of micafungin [Figure 7C].

Mono-infection DC. Finally, we performed single strain infections in which mice were inoculated intravenously with either bar-coded M1 or M2 ($1x10^6$ CFU). M1 burdens were significantly higher than M2 burdens within kidneys at d1 and 3 [Supplemental Figure 5]. Both strains were mixtures of yeast and filamentous morphologies within kidneys [Supplemental Figure 6].

Tri7 strains in longitudinal and spiked BCs. Echinocandin treatment in patient MN was initiated on d2. To estimate point prevalence, we screened 96 strains from longitudinal BCs for attenuated biofilm formation (< 30% of that formed by euploid strain M2) as marker for Tri7 and confirmed results for certain strains by qPCR. Percentages of Tri7 strains were 74% (baseline, 71/96), 7% (d3, 7/96), 2% (d5, 2/96), 2% (d10, 2/96) and 0% (d13, 0/96) [Supplemental Figure 3].

To assess Tri7 stability, we spiked M1 into a sterile BC bottle and incubated at 37ºC until turbidity was evident (24-48h). Aliquots were sub-cultured on SDA plates at 30ºC for 48h, and each of 10 strains from randomly selected colonies was shown to still harbor Tri7 by WGS [Supplemental Figure 7].

Discussion.

We demonstrated that *C. albicans* strains from BCs of individual patients were genetically and phenotypically diverse. The most striking within-patient genetic differences among strains were aneuploidies and LOH, which were identified in 3 of 4 patients. In patient

MN, Tri7 and euploid strains were equally fit in liquid media, and they exhibited similar micafungin MICs. Euploid strains, however, were more tolerant to micafungin than Tri7 strains by FoG, SMG and competitive growth assays. In contrast, Tri7 strain M1 was more fit than euploid strain M2 during growth in human blood ex vivo, and during mouse models of GI colonization and DC. M2 was more competitive than M1 in mouse kidneys following micafungin treatment of DC than it was in the absence of micafungin. Tri7 strains predominated in patient MN's baseline BC (74% of the population), but they were largely replaced by euploid strains after 1 and 3d of echinocandin treatment (93% and 98% euploid, respectively). By d13 of BSI, 100% of BC strains were euploid. The data suggest that Tri7 strains were more virulent than euploid strains, which conferred an advantage at baseline in absence of antifungal treatment. Echinocandin tolerant, euploid strains that were present at baseline but unrecognized by the clinical lab emerged as dominant upon echinocandin exposure. These results and our previous findings for *C. glabrata*- and CRKP-positive BCs challenge the single organism hypothesis of BSI pathogenesis, and they support a population-based paradigm for BSIs by commensal microbes in at least some patients.[12,13]

Large-scale genetic variants like aneuploidy and LOH, including Tri7, are described in clinical *C. albicans* strains and in strains exposed to antifungals in vitro or recovered from mouse models of candidiasis.[5,15,19-22] Aneuploidy can involve any *C. albicans* Chr, with positive or negative consequences for fitness and antifungal susceptibility depending on specific Chr, strain background and environmental conditions.[23-25] Findings that Tri7 strain M1 was attenuated for hyphal formation in vitro compared to euploid partner strain M2, while exhibiting enhanced GI colonization, invasion of ileum and colon, and hematogenous infection of kidneys in mice, were consistent with data for certain previously studied Tri7 strains.[15,22,25] Echinocandin tolerance has been described for *C. albicans* strains with Chr2 and Chr5 aneuploidies, but it has not been associated with Tri7.[26-30] Fluconazole tolerance has been reported in some *C.*

albicans strains causing persistent BSIs despite treatment,[16] but neither fluconazole nor echinocandin tolerance are broadly validated as determinants of outcomes in infected patients.[16 26,30] We did not identify echinocandin-resistant *C. albicans* strains. In our *C. glabrata* study, baseline BCs in 2 of 10 patients were a mixture of fluconazole-susceptible and originally unrecognized fluconazole-resistant strains, the latter of which were later recovered as index strains from recurrent infections. Recently, echinocandin heteroresistance (a low-frequency subpopulation of resistant cells) among *C. parapsilosis* was connected to echinocandin break-through BSIs.[31] There is pressing need for multicenter studies of the clinical relevance of pheno-types like antifungal tolerance and heteroresistance that are not detected by standard clinical laboratory susceptibility testing methods.

As is true for antifungal tolerance, the clinical relevance of diversity in virulence among *Candida* strains is uncertain. While hyphal and biofilm formation are classic *C. albicans* virulence determinants, it is more precise to understand bidirectional regulation of morphogenesis and biofilm maturation, as dictated by local environment, as crucial to commensalism and pathogenesis.[32] It is well recognized that certain *C. albicans* strains, like Tri7 strains here, manifest filamentation defects on solid agar, but not in liquid media or within target organs. Moreover, strains with attenuated filamentation or biofilm formation in vitro may manifest full or even heightened pathogenic capacity in vivo. In the end, *C. albicans* is an opportunistic pathogen that does not depend upon a dominant virulence factor, but rather a complex interplay of properties that optimize survival in various in vivo niches.[14] At least in part, attenuated hyphal formation by Tri7 strains in vitro has been attributed here and elsewhere to over-expression of *NRG1*, which was initially described as a transcriptional repressor of *C. albicans* SC5314 hyphal and stress response genes.[15] It is now apparent that *NRG1* exerts variable effects on gene expression, filamentation, fitness and virulence depending on strain background.[15,33,34] Tri7 was not previously linked to aberrant *C. albicans* biofilm formation,

although high *NRG1* expression was shown to limit biofilm maturation and promote dispersion of yeast cells from immature biofilm.[35]

Tri7 was stable in strain M1 following incubation in spiked BC bottles, suggesting that euploid strains in patient MN emerged in vivo rather than ex vivo. This finding is notable since changes in *Candida* ploidy are often reversible adaptations to stress.[36] We propose that most of the *C. albicans* and *C. glabrata* strain diversity we observed in BCs was likely to have arisen during GI commensalism (or at another colonization site).[6] We recognize that we may have failed to identify important genetic or phenotypic variants by studying only 10 *Candida* strains per patient. It is feasible that *C. albicans* genetic variants other than differences in Chr7 ploidy also contribute to important phenotypes. In our previous study, the predominant within-patient genetic differences among *C. glabrata* strains from baseline BCs of 10 patients were core genome SNPs and indels.[12] Within-patient SNPs and indels were less prevalent among *C. albicans* strains from BCs of 4 patients. Future studies will elaborate whether differences between spp. have biologic explanations, reflect features that are particular to individual cases, and/or stem from relatively small sample sizes. To date, our studies are the only investigations of within-patient diversity among *Candida* strains during BSIs. Results cannot necessarily to extrapolated to other *Candida* spp., other opportunistic commensal microbes, or other sites of infection.

In conclusion, positive BCs contained mixed populations of *C. albicans* strains that differed most strikingly by aneuploidies and LOH, and in echinocandin tolerance and virulence attributes. Studies to assess the clinical relevance of *Candida* diversity are indicated, as is research into understanding how diversity and adaptation of various microbes facilitates commensalism and disease. If results here and from our studies of *C. glabrata* and CRKP BSIs are validated, clinical and microbiology lab practices may need to be revised to consider microbial populations.

Methods.

This study was approved by the University of Pittsburgh Institutional Review Board through Expedited Review according to OHRP, 45 CFR 46.110 and FDA 21 CFR 56.110, and by the University of Pittsburgh Animal Care and Use Committee. Reagents, primers and plasmids appear in Supplemental Tables 3, 4 and 5, respectively. BC bottles and index strains from patients with *C. albicans* BSI were obtained from the UPMC clinical microbiology laboratory.[12] We streaked 10 µL from bottles onto 2 SDA plates and incubated for 48h at 35°C. For each BC, a strain isolated from each of 4–9 morphologically indistinguishable colonies and the index strain underwent Illumina NextSeq WGSing [Supplemental Table 4].

Illumina NextSeq and bioinformatic analysis. DNA extraction, library preparation and genome analysis were performed as previously published,[12] and as described with details of variant filtration in Supplemental Methods.[37-41] We selected gene variants called in ≥ 1 strain, but not all strains within each patient, focusing on non-synonymous substitutions, disrupted start/stop codons, and frameshift indels. Aneuploidy, gene deletions/duplications and LOH were analyzed using Ymap [42] and reference genome SC5314 (CGD: A21-s02-m09-r10). We used allelic ratio (homozygous: 0 or 1; heterozygous: 0.5) to determine whether a region with SNPs in the parent/reference strain had undergone LOH. Allelic ratio was calculated for each coordinate as: (number of reads with the more abundant base call)/(total number of reads). We selected internal strains for each patient to create a haplotype map and investigate within-patient LOH.

In vitro phenotypes. Growth rate, filamentation, antifungal susceptibility, micafungin tolerance, dot blot and biofilm assays were performed using well-established protocols, as described in detail in Supplemental Methods.[16,17,43]

Chromosome copy numbers. Chr5 and Chr7 copy numbers were determined by qPCR using multiple primer pairs, as previously described [Supplemental Table 5]. Chr1 and Chr4 qPCRs were copy number controls.[14]

qRT-PCR transcriptional analysis was performed using SYBR Green qPCR Master Mix.[15] Expression was calculated using ΔΔCT, with normalization to housekeeping genes *ACT1* and 18S rDNA.

***NRG1* over-expression strain.** The *NRG1* promoter was replaced with the constitutively expressed *TDH3* promoter from plasmid pCJN542 (provided by Aaron Mitchell).[44] Euploid strains M2 and N1 were transformed using PCR products from pCJN542 and primers NRG1-OE-F and NRG1-OE-R. Overexpression strains were selected on YPD+clonNAT (YPD, 200 µg/mL nourseothricin sulfate) plates.

Barcoded strains were constructed as previously described.[15] Plasmids RB793 (Addgene #199121) and RB794 (Addgene #199122) containing barcodes were digested with NgoMIV and transformed into target strains. Transformants were selected on YPD+200 µg/mL nourseothricin. Integration at *NEUT5L* was confirmed by PCR using primers in Supplemental Table 4.

In vitro competitive growth. Barcoded strains were grown overnight in liquid YPD at 30□C, washed with PBS and diluted in YPD. Strains (1:1 ratio, $1x10^4$ CFU/mL each) were incubated at 39ºC with shaking (200rpm). Micafungin (0.125 µg/mL) or H_2O_2 (1 mM) were added on d0, 3 and 6. On d0, 3, 6 and 9, DNA was extracted from 200µL aliquots for bar code sequencing.

GI colonization model. We used 8 mice at each time point (equal male:female, 4-6 weeks old, 20-25 g, ICR CD1, Envigo). GI infections were performed as previously described.[15] Four days before infection, drinking water was supplemented with 1.5mg/mL ampicillin, 2mg/mL streptomycin and 2.5% glucose. Mice were gavaged with $1X10^8$ CFU of each strain. Fecal pellets from d1, 3, and 7 were homogenized in sterile PBS. On d7, stomach, ileum and colon were homogenized in PBS. Homogenates were plated on SDA plates with 200µg/mL each of ampicillin, streptomycin, chloramphenicol, kanamycin and nourseothricin, and processed for DNA extraction.[15]

DC model. We intravenously inoculated 6 and 8 mice (equal male:female) per time point for co-infections and mono-infections, respectively; inocula were $5x10^5$ CFU per barcoded strain (co-infection) or $1x10^6$ CFU (mono-infection). In co-infections, an additional 6 mice were treated with micafungin (8.3 mg/kg/mouse intraperitoneal, 30 minutes post-infection) and sacrificed at 24h. Kidneys were homogenized for DNA extraction and barcode sequencing on d1, 3 and 7 post-infection (co-infection), or for tissue burden determination on SDA (mono-infection).[15]

Barcode sequencing. DNA (1-3 µL) extracted from in vitro experiments, fecal samples and organ homogenates (Zymobiomics DNA Miniprep kit; Zymo Research) was used for PCR[14] [Supplemental Table 4]. PCR parameters were 98°C for 30s, 98°C for 10s, 60°C for 30s, 72°C for 30s; steps 2 to 4 repeated for 34 cycles; and 72°C for 5 min. PCR products were gel purified (Wizard SV gel and PCR clean-up system, Promega). ExpressPlex library preparation and sequencing was done by SeqWell (MA, USA). Strains were identified by unique barcode using CLC Genomic workbench v.22.0.1. BC1/BC2 ratio was calculated and normalized by initial inoculum. BC2 percent was calculated as: (1/(Ratio+1))X100%.

Populations in longitudinal BC bottles. Ninety-six strains from each BC in patient MN were screened for attenuated biofilm formation as a marker for Tri7 (mean biofilm OD_{590} of 3 independent experiments <30% of mean biofilm formed by euploid strain M2). Ploidy was confirmed by qPCR for ≥ 10 strains from each of d0 and d13 BCs.

BC bottle spiking. A single colony of Tri7 M1 suspended in 50 µl saline was inoculated into a sterile BC bottle (Fisher Scientific BD BACTEC Plus Aerobic medium BD442023) that contained 5 mL blood from a healthy volunteer (~1 CFU/mL), and incubated at 37°C with shaking (225rpm) until turbidity was evident.[12] Ten microliters were streaked on an SDA plate, and incubated at 30°C for 48h. Single strains were isolated from 5-10 randomly chosen colonies for DNA extraction and Illumina sequencing.

Statistical analyses were performed using GraphPad Prism v9.1.2. Symmetric and asymmetric data are presented as means and standard error and as medians and interquartile ranges,

respectively. CFU/g were log-transformed prior to analysis. Student t-test or Mann-Whitney U tests were used for comparisons of 2 groups, and one-way ANOVA or Kruskal-Wallis for comparisons of >2 groups. For all analyses, $p<0.05$ (two-tailed) was significant.

Data availability. Datasets are available in data files submitted with this article. WGS data have been deposited in the NCBI database under accession number PRJNA1118730. BioProject and associated SRA metadata are at: https://dataview.ncbi.nlm.nih.gov/object/PRJNA1118730?reviewer=nuvb3aprq91400u9pri6s57r97

Acknowledgements. This project was supported by VA Merit Review 1IO1BX001955 (Dr. Clancy) and NIH R21 AI160098 (Dr. Nguyen) awards. Some of the data were presented at IDWeek 2024 (October 14, 2024, Los Angeles, CA). The authors do not report any conflicts of interest.

References.

1. Sitterlé E, Maufrais C, Sertour N, Palayret M, D'Enfert C, Bougnoux M-E. Within-Host Genomic Diversity of Candida albicans in Healthy Carriers. Scientific Reports 2019;9.
2. Anderson FM, Visser ND, Amses KR, et al. Candida albicans selection for human commensalism results in substantial within-host diversity without decreasing fitness for invasive disease. PLOS Biology 2023;21:e3001822.
3. Gabaldon T, Carrete L. The birth of a deadly yeast: tracing the evolutionary emergence of virulence traits in Candida glabrata. FEMS Yeast Res 2016;16:fov110.
4. Hickman MA, Zeng G, Forche A, et al. The 'obligate diploid' Candida albicans forms mating-competent haploids. Nature 2013;494:55-9.
5. Hirakawa MP, Martinez DA, Sakthikumar S, et al. Genetic and phenotypic intra-species variation in *Candida albicans*. Genome Research 2015;25:413-25.
6. Carreté L, Ksiezopolska E, Gómez-Molero E, et al. Genome Comparisons of Candida glabrata Serial Clinical Isolates Reveal Patterns of Genetic Variation in Infecting Clonal Populations. Frontiers in Microbiology 2019;10.
7. Munoz JF, Gade L, Chow NA, et al. Genomic insights into multidrug-resistance, mating and virulence in Candida auris and related emerging species. Nat Commun 2018;9:5346.
8. Didelot X, Walker AS, Peto TE, Crook DW, Wilson DJ. Within-host evolution of bacterial pathogens. Nat Rev Microbiol 2016;14:150-62.
9. Moxon ER, Murphy PA. Haemophilus influenzae bacteremia and meningitis resulting from survival of a single organism. Proc Natl Acad Sci U S A 1978;75:1534-6.
10. Rubin LG. Bacterial colonization and infection resulting from multiplication of a single organism. Rev Infect Dis 1987;9:488-93.
11. Young BC, Wu CH, Gordon NC, et al. Severe infections emerge from commensal bacteria by adaptive evolution. Elife 2017;6.
12. Badrane H, Cheng S, Dupont CL, et al. Genotypic diversity and unrecognized antifungal resistance among populations of Candida glabrata from positive blood cultures. Res Sq 2023.
13. Cheng S, Fleres G, Chen L, et al. Within-Host Genotypic and Phenotypic Diversity of Contemporaneous Carbapenem-Resistant Klebsiella pneumoniae from Blood Cultures of Patients with Bacteremia. mBio 2022;13:e0290622.
14. Katsipoulaki M, Stappers MHT, Malavia-Jones D, Brunke S, Hube B, Gow NAR. Candida albicans and Candida glabrata: global priority pathogens. Microbiol Mol Biol Rev 2024;88:e0002123.
15. Kakade P, Sircaik S, Maufrais C, Ene IV, Bennett RJ. Aneuploidy and gene dosage regulate filamentation and host colonization by *Candida albicans*. Proceedings of the National Academy of Sciences 2023;120.
16. Rosenberg A, Ene IV, Bibi M, et al. Antifungal tolerance is a subpopulation effect distinct from resistance and is associated with persistent candidemia. Nat Commun 2018;9:2470.
17. Berman J, Krysan DJ. Drug resistance and tolerance in fungi. Nat Rev Microbiol 2020;18:319-31.
18. Rottmann M, Dieter S, Brunner H, Rupp S. A screen in Saccharomyces cerevisiae identified CaMCM1, an essential gene in Candida albicans crucial for morphogenesis. Mol Microbiol 2003;47:943-59.
19. Anderson MZ, Saha A, Haseeb A, Bennett RJ. A chromosome 4 trisomy contributes to increased fluconazole resistance in a clinical isolate of Candida albicans. Microbiology 2017;163:856-65.
20. Selmecki A, Gerami-Nejad M, Paulson C, Forche A, Berman J. An isochromosome confers drug resistance *in vivo* by amplification of two genes, *ERG11* and *TAC1*. Molecular Microbiology 2008;68:624-41.
21. Yang F, Todd RT, Selmecki A, Jiang Y-Y, Cao Y-B, Berman J. The fitness costs and benefits of trisomy of each *Candida albicans* chromosome. Genetics 2021;218.
22. Ene IV, Farrer RA, Hirakawa MP, Agwamba K, Cuomo CA, Bennett RJ. Global analysis of mutations driving microevolution of a heterozygous diploid fungal pathogen. Proceedings of the National Academy of Sciences 2018;115:E8688-E97.
23. Forche A, Cromie G, Gerstein AC, et al. Rapid Phenotypic and Genotypic Diversification After Exposure to the Oral Host Niche in *Candida albicans*. Genetics 2018;209:725-41.
24. Forche A, Solis NV, Swidergall M, et al. Selection of Candida albicans trisomy during oropharyngeal infection results in a commensal-like phenotype. PLOS Genetics 2019;15:e1008137.
25. Tso GHW, Reales-Calderon JA, Tan ASM, et al. Experimental evolution of a fungal pathogen into a gut symbiont. Science 2018;362:589-95.

26. Yang F, Berman J. Beyond resistance: antifungal heteroresistance and antifungal tolerance in fungal pathogens. Current Opinion in Microbiology 2024;78:102439.
27. Yang F, Gritsenko V, Slor Futterman Y, et al. Tunicamycin Potentiates Antifungal Drug Tolerance via Aneuploidy in Candida albicans. mBio 2021;12.
28. Yang F, Teoh F, Tan ASM, Cao Y, Pavelka N, Berman J. Aneuploidy Enables Cross-Adaptation to Unrelated Drugs. Molecular Biology and Evolution 2019;36:1768-82.
29. Yang F, Zhang L, Wakabayashi H, et al. Tolerance to Caspofungin in Candida albicans Is Associated with at Least Three Distinctive Mechanisms That Govern Expression of *FKS* Genes and Cell Wall Remodeling. Antimicrobial Agents and Chemotherapy 2017;61:AAC.00071-17.
30. Suwunnakorn S, Wakabayashi H, Rustchenko E. Chromosome 5 of Human Pathogen Candida albicans Carries Multiple Genes for Negative Control of Caspofungin and Anidulafungin Susceptibility. Antimicrobial Agents and Chemotherapy 2016;60:7457-67.
31. Zhai B, Liao C, Jaggavarapu S, et al. Antifungal heteroresistance causes prophylaxis failure and facilitates breakthrough Candida parapsilosis infections. Nat Med 2024.
32. Saville SP, Lazzell AL, Monteagudo C, Lopez-Ribot JL. EngineeredControl of Cell Morphology In Vivo Reveals Distinct Roles for Yeast andFilamentous Forms of *Candida albicans* duringInfection. Eukaryotic Cell 2003;2:1053-60.
33. Mao Y, Solis NV, Filler SG, Mitchell AP. Functional Dichotomy for a Hyphal Repressor in Candida albicans. mBio 2023;14:e0013423.
34. Wakade RS, Wellington M, Krysan DJ. The role of the C. albicans transcriptional repressor NRG1 during filamentation and disseminated candidiasis is strain dependent. mSphere 2024;9:e0078523.
35. Uppuluri P, Pierce CG, Thomas DP, Bubeck SS, Saville SP, Lopez-Ribot JL. The Transcriptional Regulator Nrg1p Controls Candida albicans Biofilm Formation and Dispersion. Eukaryotic Cell 2010;9:1531-7.
36. Anderson MZ, Dietz SM. Evolution and strain diversity advance exploration of Candida albicans biology. mSphere 2024;9:e0064123.
37. McKenna A, Hanna M, Banks E, et al. The Genome Analysis Toolkit: A MapReduce framework for analyzing next-generation DNA sequencing data. Genome Research 2010;20:1297-303.
38. Cingolani P, Platts A, Wang LL, et al. A program for annotating and predicting the effects of single nucleotide polymorphisms, SnpEff. Fly 2012;6:80-92.
39. Danecek P, Bonfield JK, Liddle J, et al. Twelve years of SAMtools and BCFtools. GigaScience 2021;10.
40. Kozlov AM, Darriba D, Flouri T, Morel B, Stamatakis A. RAxML-NG: a fast, scalable and user-friendly tool for maximum likelihood phylogenetic inference. Bioinformatics 2019;35:4453-5.
41. Letunic I, Bork P. Interactive Tree Of Life (iTOL) v5: an online tool for phylogenetic tree display and annotation. Nucleic Acids Research 2021;49:W293-W6.
42. Abbey DA, Funt J, Lurie-Weinberger MN, et al. YMAP: a pipeline for visualization of copy number variation and loss of heterozygosity in eukaryotic pathogens. Genome Medicine 2014;6.
43. Institute CaLS. Reference Method for Broth Dilution Antifungal Susceptibility Testing of Yeasts. 4th ed. CLSI standard M27. Wayne, PA: Clinical and Laboratory Standards Institute; 2017.
44. Nobile CJ, Solis N, Myers CL, et al. Candida albicans transcription factor Rim101 mediates pathogenic interactions through cell wall functions. Cell Microbiol 2008;10:2180-96.

Figure 1. **Core genome single nucleotide polymorphism (SNP) phylogeny of *Candida albicans* strains from patients with bloodstream infections.** Ten strains from each of 4 patients (AB (magenta), MN (blue), QR (yellow) and G (green) underwent whole genome sequencing. The phylogenetic tree was built using RaxML under the general time-reversible model with 1,000-bootstrap replicates. Within-patient strains had the following ranges of SNP differences: patient AB (range, 0-7); patient MN (range, 3- 36); patient QR (range, 8-28); patient G (range, 7-42). Nodes grouping by clade and patient had 100% bootstrap support values.

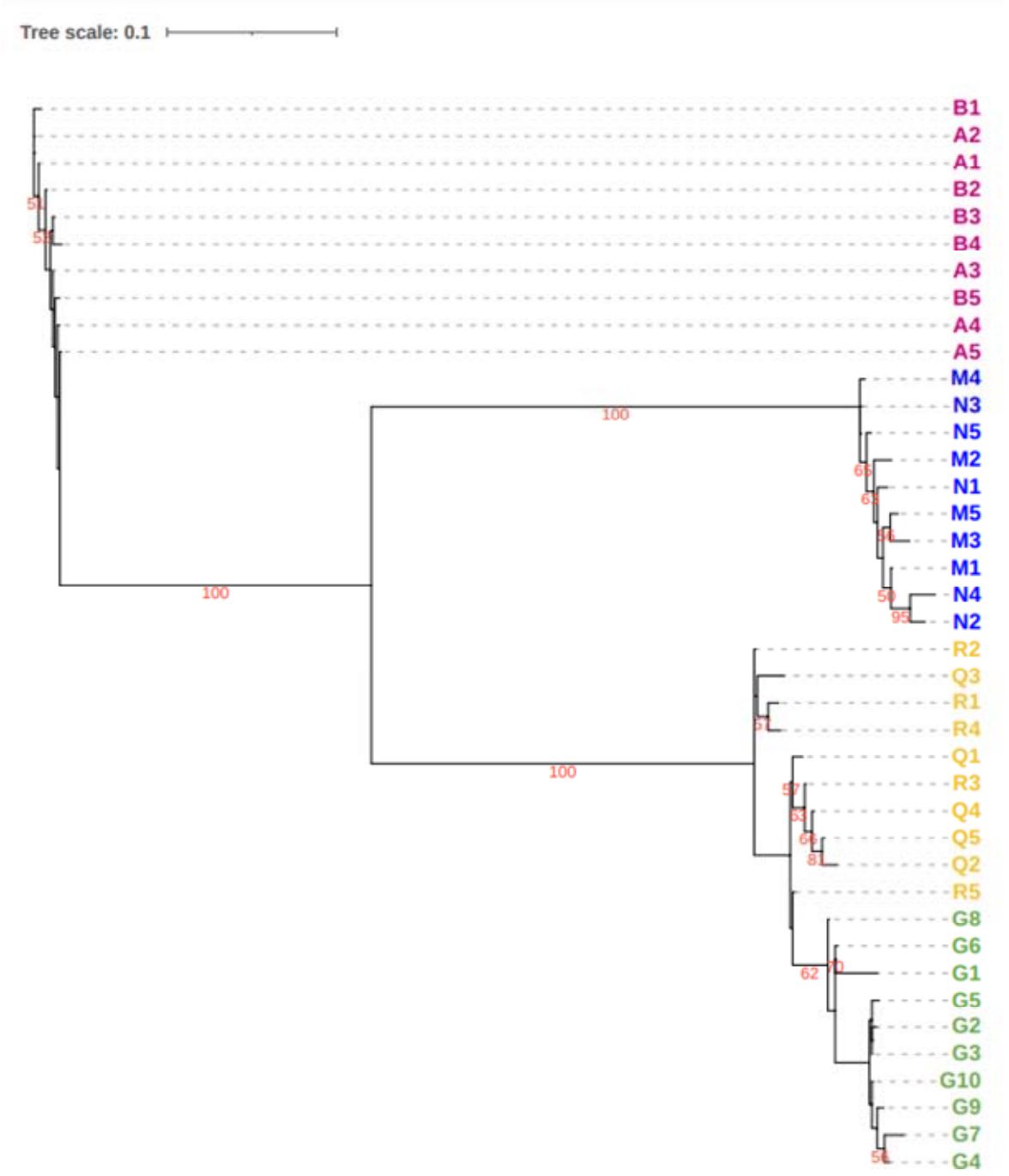

Figure 2. Copy number variants (CNVs), single nucleotide polymorphism (SNP) density and loss of heterozygosity (LOH) in *Candida albicans* strains from patients with bloodstream infections. Strains from patients G, MN and QR are shown in Figures A through C, respectively. Chromosomes are arranged along the horizontal (x) axis. The vertical (y) axis represents sequence read depth, scaled to actual copy number. CNVs are presented as black lines drawn upwards or downwards from the mid-line of the chromosome. Regions with CNV are highlighted in green. Regions of SNP density are presented as shades of grey, and homozygous regions are white. Regions of LOH are red. Black circles along the bottom of chromosomes represent major repeat sequences (MRSs). **A.** Strain G1 differed from other G strains by having an extra copy of whole Chr5 (i.e., trisomy 5), as evident by a block of black lines extending upward from the mid-line (green highlight). Strains did not differ by SNP density or LOH. **B.** Strains M1, M3, M4 and M5 differed from other MN strains by having an extra copy of whole Chr7 (i.e., trisomy 7). All MN strains had an extra copy of a small region adjacent to the second MRS of Chr7 (green highlight). Strains did not differ by SNP density or LOH. **C.** Strains Q1, Q2 and R1-R5 had a region of LOH (red highlight) in a segment at the end of the left arm of chromosome 1, which was not apparent in strains Q3-Q5. As indicated by grey highlight, the latter strains did not have gaps in SNP density in the region of LOH. A small potential region of LOH was also present uniquely in strains R1-R5, demarcated by a single red line near the middle of the left arm of Chr7; the size of this region was at or very near the resolution limit for YMAP analysis (4.5 Kb). QR strains did not differ by CNV or ploidy. The only differences among strains in SNP density was in the region of LOH.

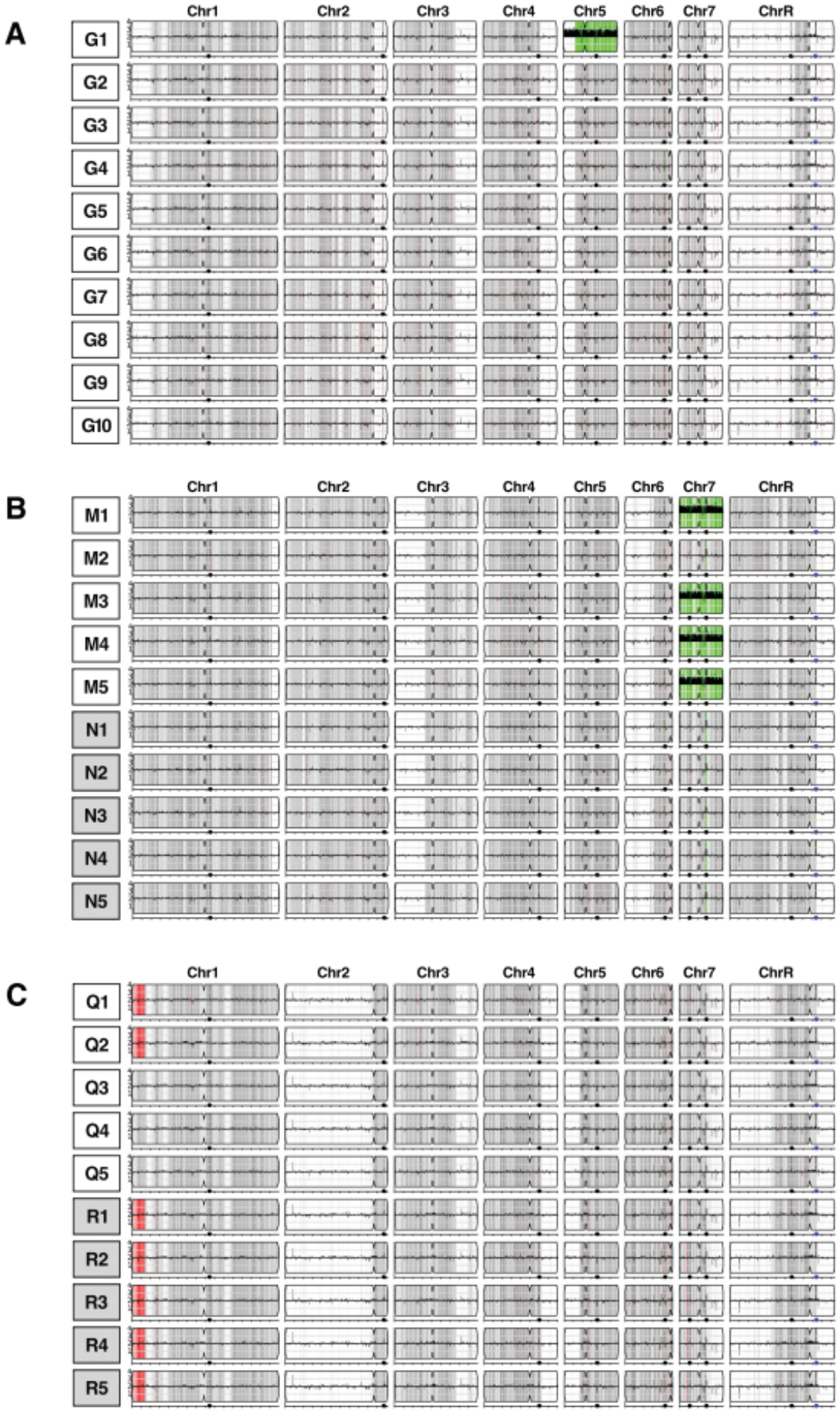
A
Chr1
Chr2
Chr3
Chr4
Chr5
Chr6
Chr7
ChrR
G1
G2
G3
G4
G5
G6
G7
G8
G9
G10
B
M1
M2
M3
M4
M5
N1
N2
N3
N4
N5
C
Q1
Q2
Q3
Q4
Q5
R1
R2
R3
R4
R5

Figure 3. Hyphal formation by MN strains on solid agar. Strains were photographed after incubation on RPMI 1640 with 2% glucose medium at 30°C for 5 days. Euploid strains (M2, N1, N2, N3, N4 and N5) formed extensive hyphae, whereas trisomy 7 strains M1, M3, M4 and M5 did not.

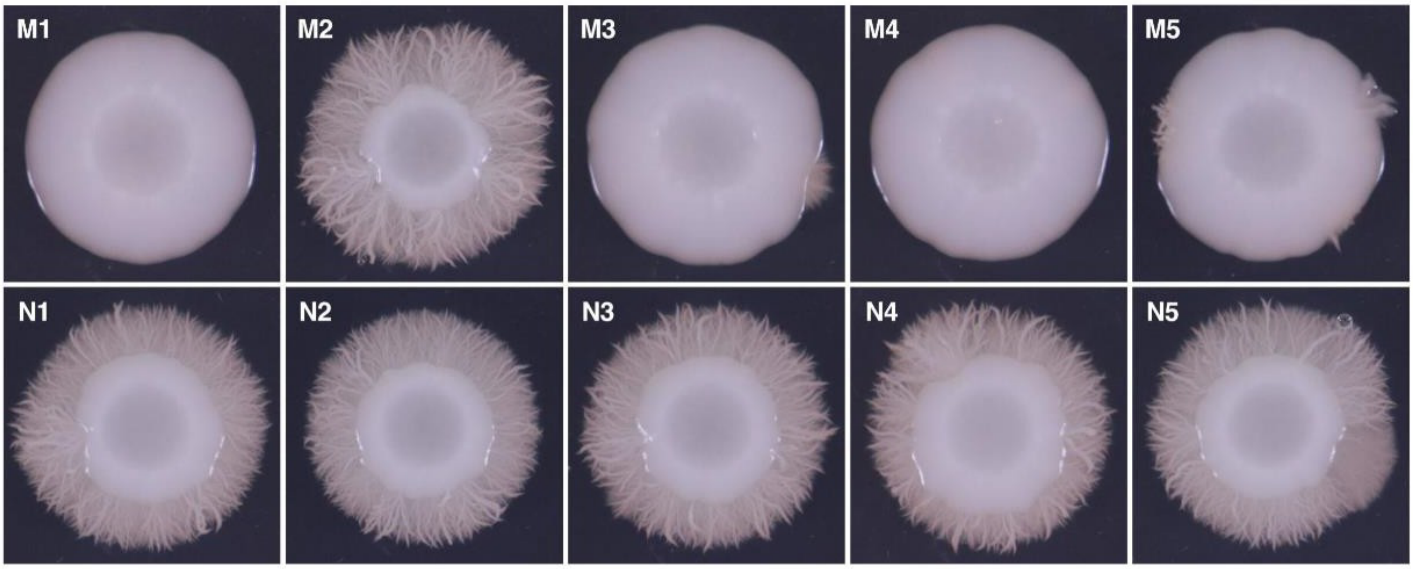

Figure 4. Biofilm formation by MN strains. Biofilm formation by MN strains at 37°C in RPMI1640 medium supplemented with 2% (w/v) glucose was measured by a 0.1% aqueous crystal violet assay in flat bottom wells as optical density at 590 nm (OD_{590}). Data are presented as mean ± SEM of ratio of OD_{590} for a given strain relative to that of euploid strain M2 (3 independent experiments). Tri7 (M1, M3, M4 and M5) and euploid (M2, N1-N5) strains are represented by striped and solid grey bar graphs, respectively. Tri7 strains consistently produced < 30% of biofilm produced by euploid strains (mean ± SEM ratio: 0.17±0.01 *vs*. 0.99±0.04; ****p<0.0001, Mann-Whitney test). Tri7 strains did not differ significantly from one another in biofilm formation, nor did euploid strains significantly differ among themselves.

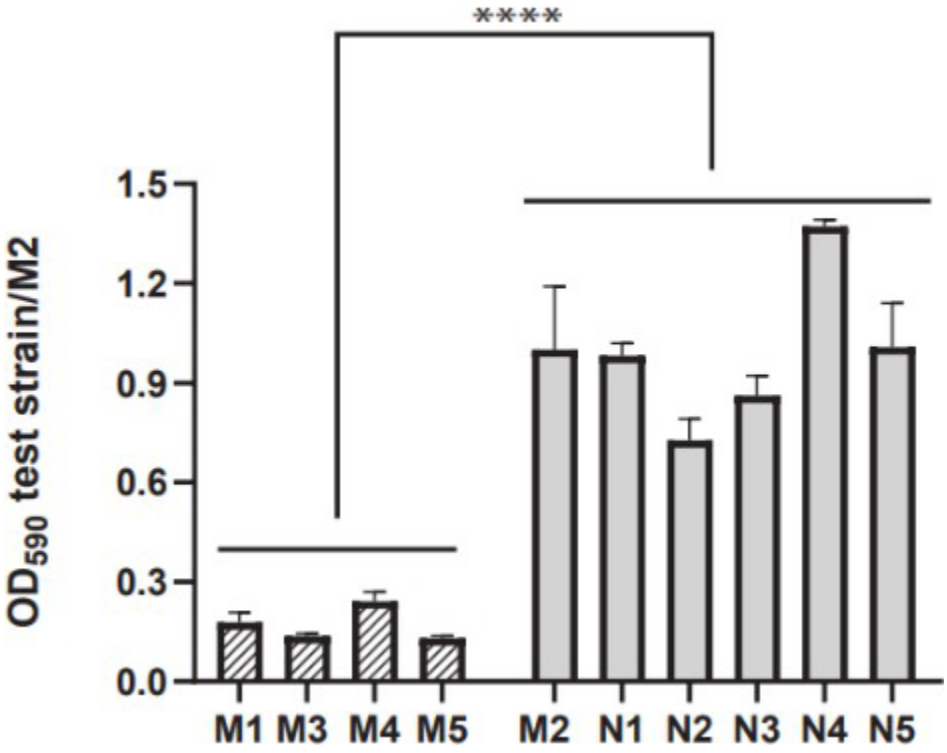

Figure 5. Susceptibility of MN strains to cell wall-active agents and tolerance to micafungin. A. In susceptibility experiments, serial 10-fold dilutions starting at $1x10^6$ CFU/mL of trisomy7 and euploid strains were spotted at exponential growth onto Sabouraud dextrose agar (SDA, control) and SDA containing Congo red (200µg/mL), sodium dodecyl sulfate (SDS, 0.04%) or micafungin (0.03 µg/mL). Plates were incubated at 30°C or 39°C for 3d. Images are shown for representative trisomy7 (M1, M3) and euploid (M2, N1) strains on d3 at 39°C. Phenotypes were similar at 30°C. **B.** Micafungin tolerance was first assessed using a disk diffusion assay to measure fraction of growth (FoG). A filter disc inoculated with 5 µg of micafungin was placed in the middle of a casitone agar place saturated with *C. albicans* strains. Tolerance was determined at 48h growth at 35°C. FoG was defined as growth within the region of inhibition relative to the maximum growth. FoG was calculated by diskImageR and image J at 80%, 50% and 20% relative inhibition (FOG_{80}, FOG_{50} and FOG_{20}, respectively). Data shown are mean ± standard error of means of FoG values for Tri7 and euploid strains. *P*-values were determined by student's t test with Welsh correction (* denotes $p < 0.05$ and ** $p<0.01$). **C.** Micafungin tolerance was also assessed using a broth microdilution assay to measure supra-MIC growth (SMG, defined as the proportion of average of growth at 48h in wells with drug concentration above the MIC relative to the growth of no drug control wells). SMG data (OD_{600} at 48h) are presented as mean ± standard error of euploid and Tri7 strains on a bar graph (top) and as a heat map (bottom). Heat map scale is shown on the bottom right.

A

B

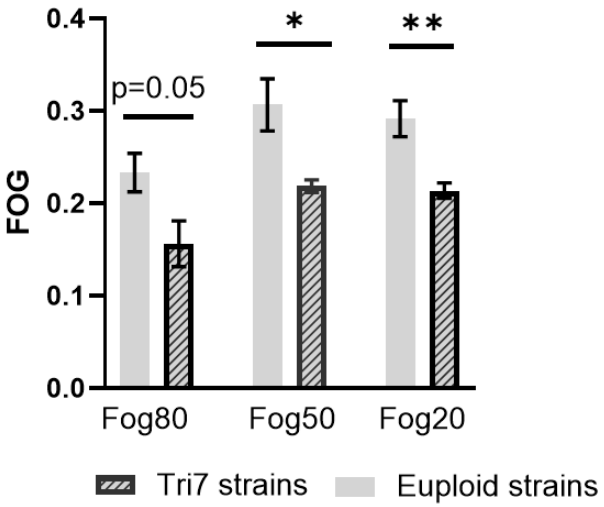

C

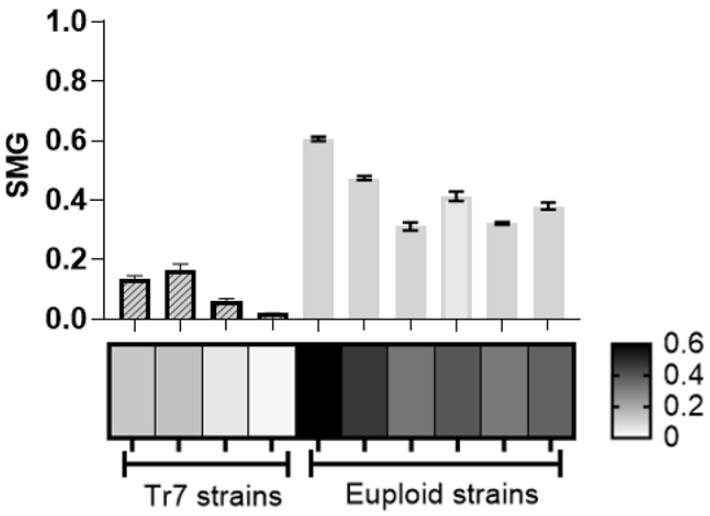

Figure 6. Competitive fitness of trisomy 7 strain M1 and euploid strain M2 in vitro and ex vivo. Barcoded strains M1 and M2 were mixed 1:1 in all experiments; input ratios were confirmed by colony forming unit determinations. At given timepoints, competitive indices (fraction of total population) of M1 and M2 were determined by barcode sequencing. Data are presented as mean ± SEM competitive indices for each strain from 3 independent experiments. * $p<0.05$, ** $p<0.01$, *** $p<0.001$, **** $p<0.0001$ **A. In vitro**. Barcoded M1 and M2 were co-cultured in yeast peptone dextrose (YPD) medium at 39°C with or without H_2O_2 (1 mM) or micafungin (0.125 µg/mL) for 3, 6 and 9d. Strains did not differ in fitness in YPD alone or in presence of H_2O_2. M1 was significantly more fit than M2 at each time point in presence of micafungin ($p< 0.0001$; unpaired student's t test). **B. Ex vivo.** Strains were co-incubated in blood from a healthy human volunteer at 37°C. Fractions of each strain out of the total population were assessed at d1, d3 and d7. Strain M1 was significantly more fit than M2 at each time point. *P*-values were calculated using one-way ANOVA with Dunnett's multiple comparisons against inoculum fraction.

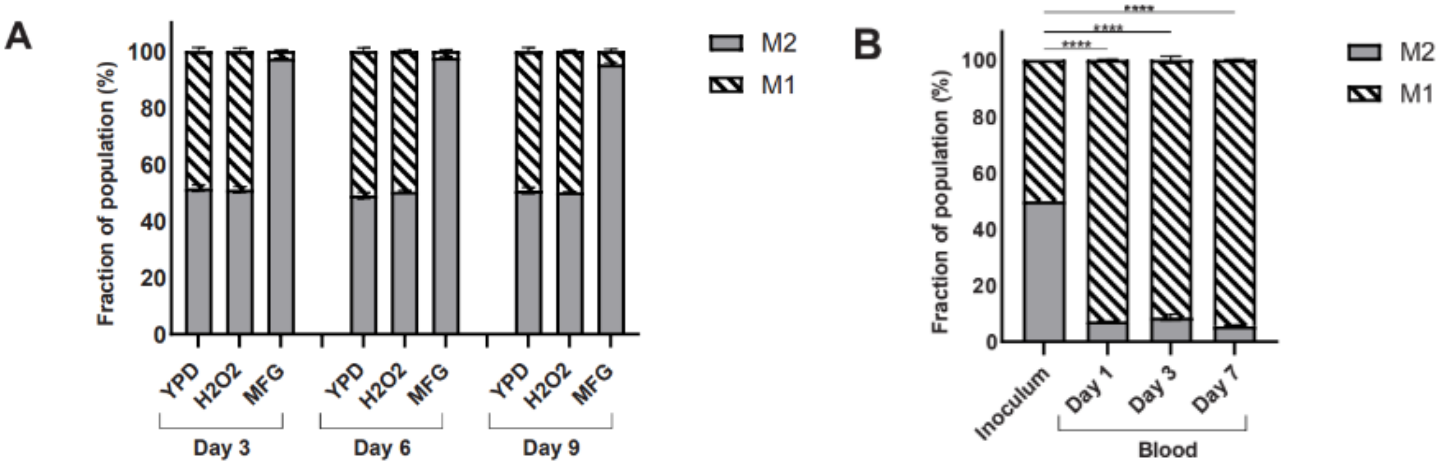

Figure 7. Competitive fitness of trisomy 7 strain M1 and euploid strain M2 in mouse models. Barcoded strains M1 and M2 were mixed 1:1 in all experiments; input ratios were confirmed by colony forming unit determinations. At given timepoints, competitive indices (fraction of total population) of M1 and M2 were determined by barcode sequencing. Data are presented as mean ± SEM competitive indices for each strain from 3 independent experiments. * $p<0.05$, ** $p<0.01$, *** $p<0.001$, **** $p<0.0001$ **A, B. Mouse model of gastrointestinal (GI) colonization**. Mice were co-infected via gavage with barcoded M1 and M2 ($1x10^8$ CFU of each strain per mouse). Stool samples were obtained on d1, d3 and d7 after inoculation (Figure 7A). On d7, mice were sacrificed, and stomach, ileum and colon were obtained and homogenized for DNA extraction for barcode sequencing (Figure 7B). M1 was significantly more fit than M2 within stool at all time points, and more fit than M2 within ileum and colon. Strains did not differ in fitness within stomachs. **C. Mouse model of disseminated candidiasis (DC).** Mice were co-infected via lateral tail vein with barcoded strains M1 and M2 ($5x10^5$ CFU of each strain per mouse). Kidneys were obtained and homogenized for DNA extraction for barcode sequencing on d1, d3 and d7. A group of co-infected mice were treated with a single dose of micafungin (8.3 mg/kg/mouse intraperitoneal, 30 minutes post-infection), and kidneys were obtained for barcode sequencing 24h following treatment. *P*-values for were determined using one-way ANOVA test with Dunn's multiple comparison against inoculum fraction. Tri7 M1 strain was more fit than M2 in the GI and DC models. M2 was significantly more fit within kidneys of mice treated with micafungin than it was within kidneys of untreated mice. NS: non-significant; MFG: micafungin

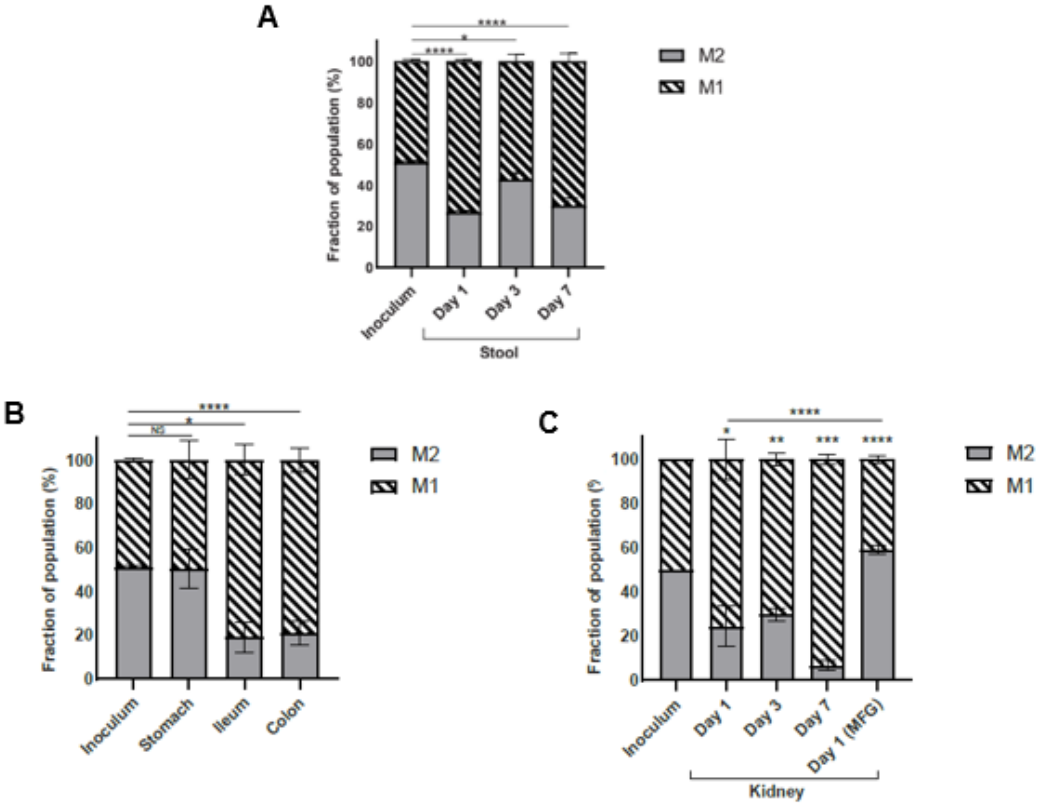

Supplemental Figure 1. Validation of trisomy of chromosomes 7 and 5 by qPCR. Chr7 and 5 copy numbers were assessed in strains from patients MN and G, respectively, by qPCR. **A.** For patient MN, 3 target regions and 2 genes (*NRG1* and *MCM1)* on Chr7 were assessed for 2 euploid (M2, N1) and 2 Tri7 (M1, M3) strains. **B.** For patient G, genes *MID1*, *MIG1* and *FAS1* on Chr5 were assessed for a euploid (G2) and a Tri5 (G1) strain. Copy numbers for strains M2, N1 and N2 and strain G1 were calculated relative to those of strains M2 or G2, respectively. Target regions of Chr1 and Chr4 were used for normalization. Data are presented as means ± SEM from 3 independent experiments. Statistical analyses were performed using ANOVA with Dunnett's (MN strains) or Sidak's (G strains) multiple comparisons tests. *P*-values <0.05 were considered significant: **p*-values <0.05, ***p*<0.01, ****p*<0.01, and ****p*<0.0001.

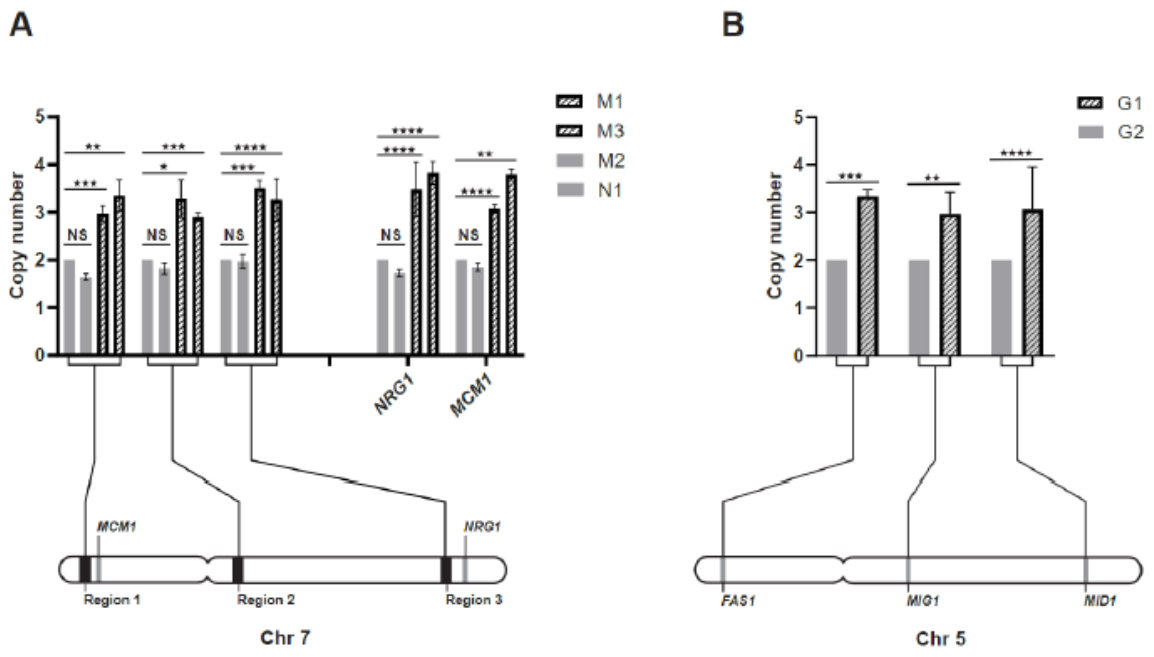

Supplemental Figure 2. Impaired hyphal formation on Spider agar medium by strains from patient G. Strains were grown under hyphal inducing conditions at 30°C. The picture here was taken after 14 days. Note lack of hyphal formation. Strains were also impaired in hyphal formation on other solid agar (M199, RPMI1640 at 30°C) and in liquid media (Yeast peptone dextrose with 10% fetal bovine serum; RPMI1640 at 37°C) (data not shown).

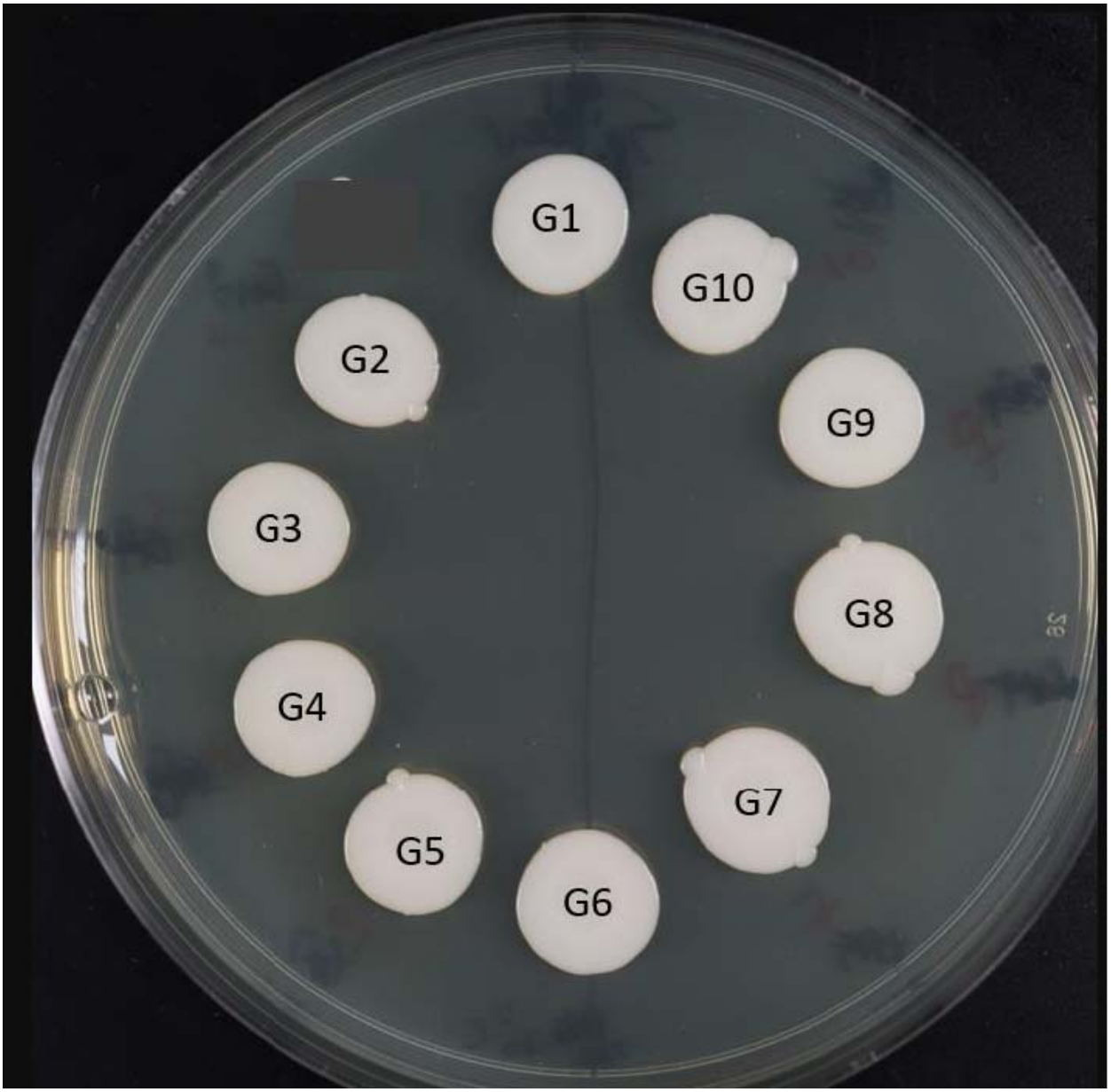

Supplemental Figure 3. Timeline of *Candida albicans*-positive blood cultures (BCs) and antifungal treatment for patient MN. The baseline positive BC (i.e., BC at time of initial diagnosis) was collected on day 0. Antifungal treatment was initiated with caspofungin on day 2, after baseline BC results were reported by the clinical microbiology lab. Subsequent BCs that were positive for *C. albicans* were collected on days 3, 5, 10 and 13. The percentage of strains from each positive BC that had trisomy of Chr7 (Tri7) is shown at the bottom of the figure and represented as black in the bar graph. The percentage of strains that were euploid for Chr7 are represented by white in the bar graph. CSP, caspofungin; FLU, fluconazole; AmB, amphotericin B

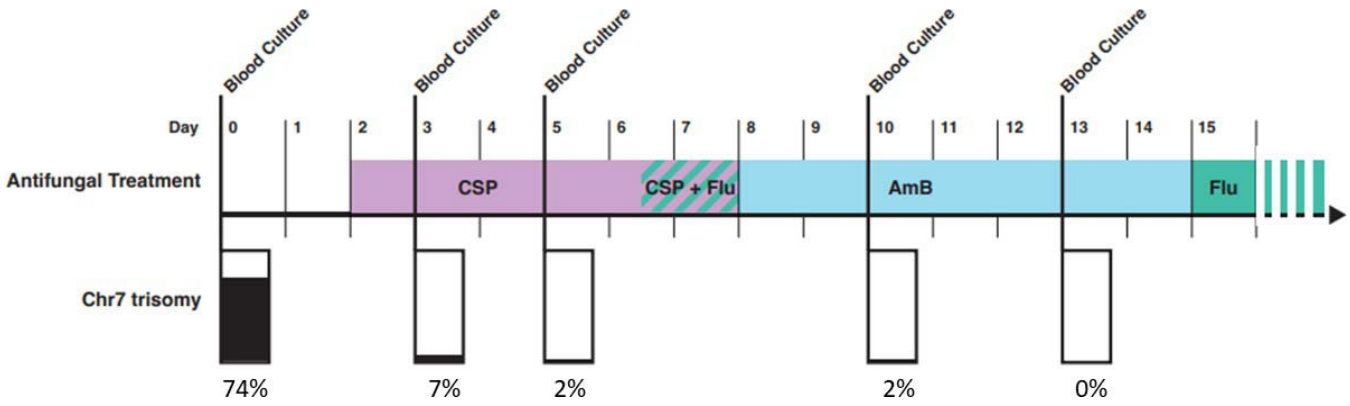

Supplemental Figure 4. Impact of *NRG1* expression on biofilm and hyphal formation. A. *NRG1* expression by Tri7 strains (M1, M3), euploid strains (N1, M2) and M2-Nrg1OE (*NRG1* over-expression strain created in M2 background) was evaluated by qRT-PCR. Expression of *PHO4* (located on Chr4) served as control. Fold differences were calculated relative to strain M2. *NRG1* expression by Tri7 strains was ~1.5-fold higher than that by euploid strains. *NRG1* expression by M2-Nrg1OE was~1.8-fold higher than that of M2. **B.** Hyphal formation by strains was assessed on RPMI1640 with 2% glucose medium. Cells at exponential stage growth were spotted onto agar plates and photographed following incubation at 30°C for 5 days. Strain M2 formed normal hyphae whereas hyphal formation by M2-Nrg1OE and M1 was attenuated. **C.** Biofilm formation was assessed using a crystal violet assay. Data in panels A and C present results from 3 independent experiments; bars represent mean ± SEM. *P*-values were calculated using ANOVA with Dunnett's multiple comparison tests, * *p*-values <0.05, ** *p* ≤0.01, *** *p*≤0.001, **** *p* ≤0.0001**.**

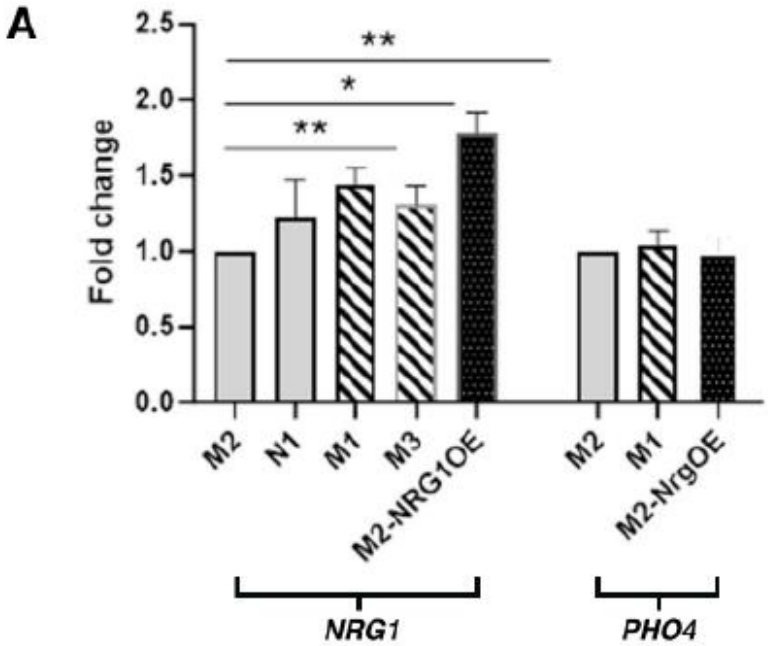

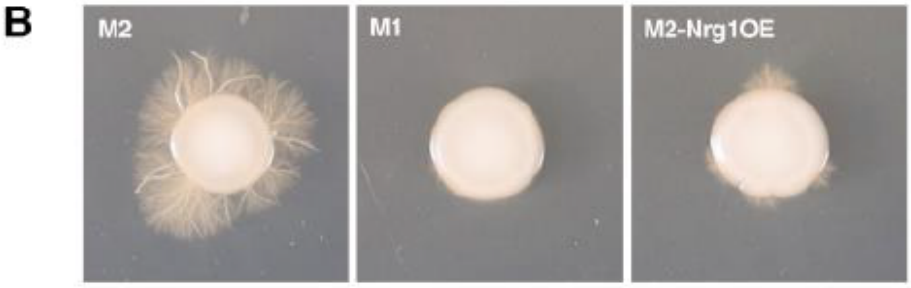

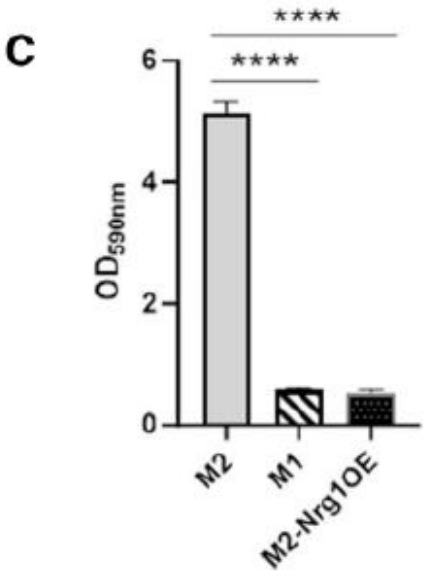

Supplemental Figure 5. Tissue burdens of strains M1 and M2 within mouse kidneys during disseminated candidiasis. Mice were infected intravenously via lateral tail vein with either bar-coded M1 or M2 ($1x10^6$ CFU). Kidneys were obtained for *C. albicans* burden enumeration. Data were log-transformed, and presented as mean ± SEM from 8 mice per strain for each timepoint. Burdens of strain M1 were significantly greater than those of strain M2 at d1 and d3 (*p*-values determined using Mann-Whitney for each timepoint).

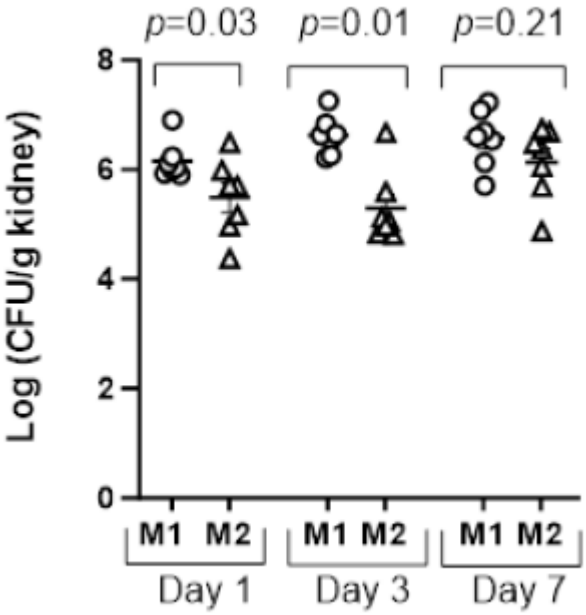

Supplemental Figure 6. Morphology of strain M1 within mouse kidneys. Kidney sections from mice infected intravenously with barcoded strains M1 or M2 alone were stained with Grocott Methenamine Silver (GMS). Strain M1 is shown growing in filamentous morphologies (denoted by arrowheads labeled with “F”) interspersed with multiple yeasts (arrowhead labeled with “Y”) (image at 400x) within kidneys on d3. Filamentous morphologies included both hyphae and pseudohyphae. M1 morphologies on d1 were similar to those on d3, and they did not differ on either day from M2 morphologies (not shown).

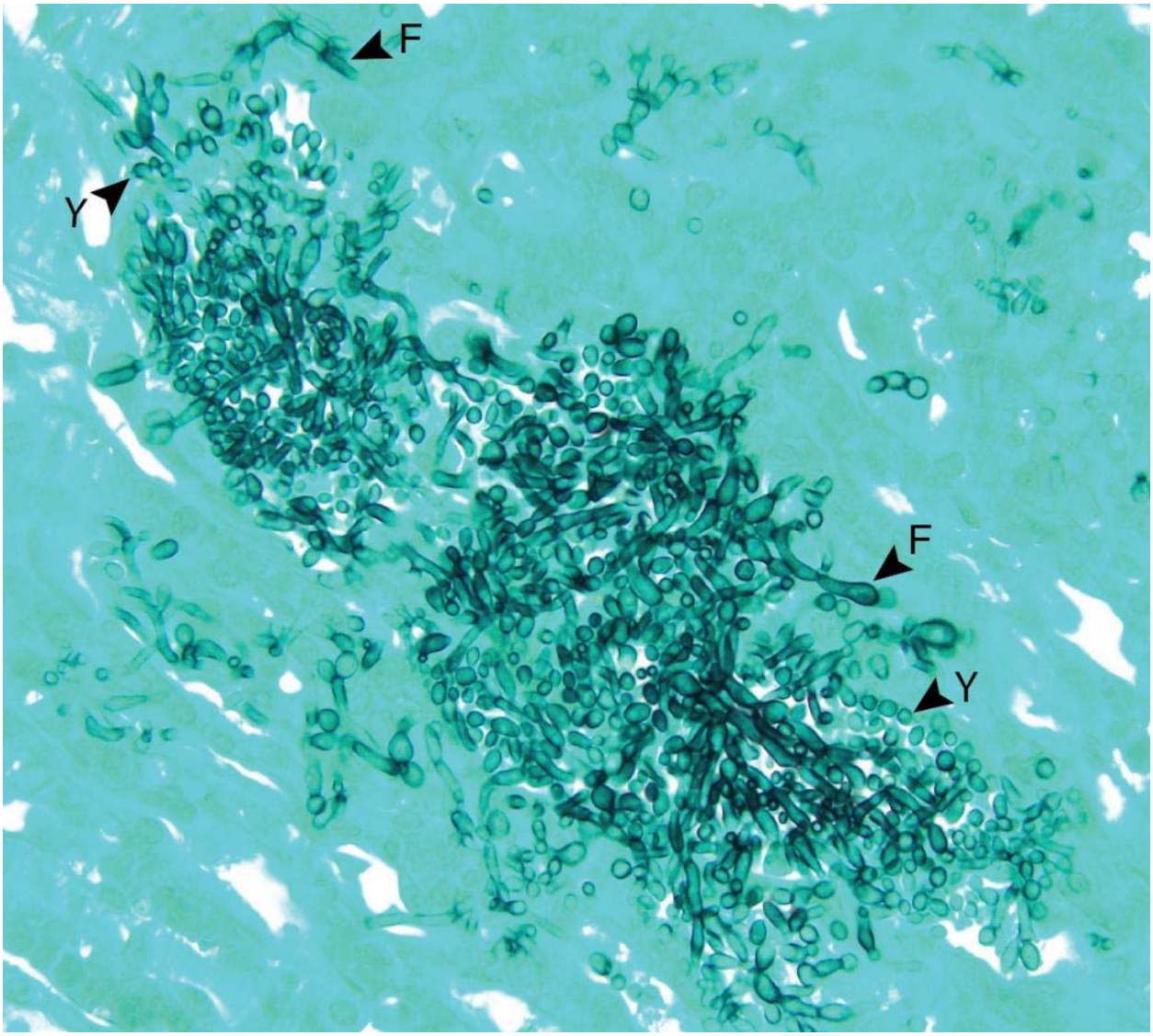

Supplemental Figure 7. Copy number variation of 10 strains isolated from a blood culture bottle spiked with M1 index strain.

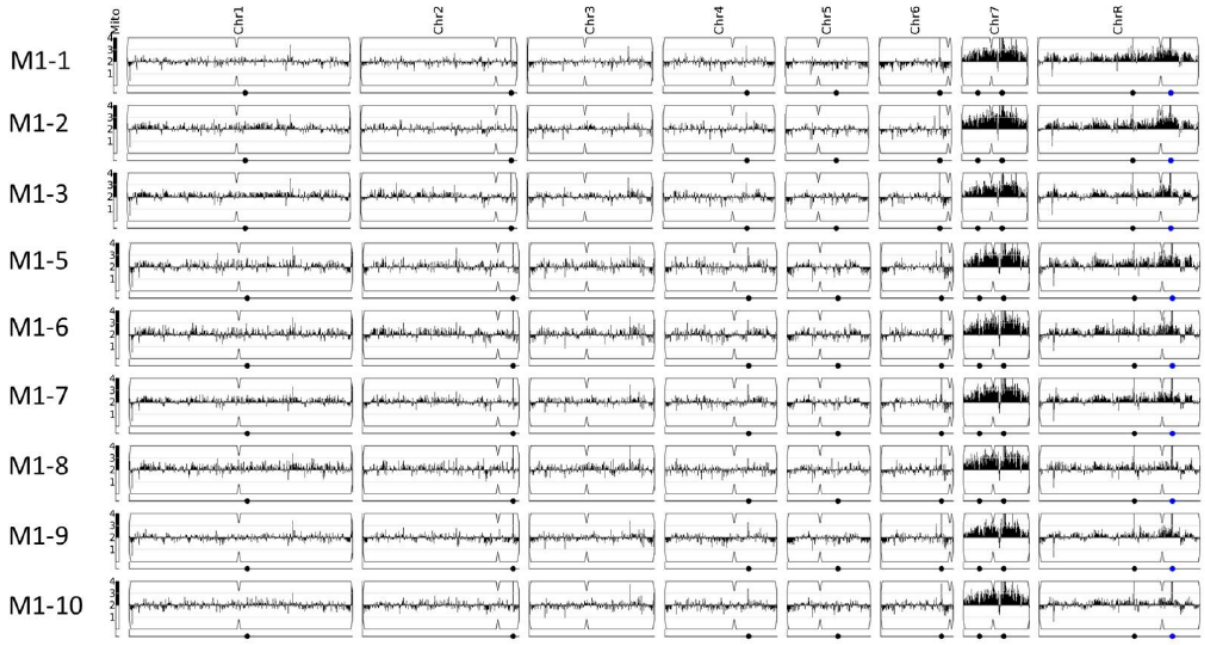

Supplemental Table 1. Clinical characteristics, treatment and outcomes of patients with *Candida albicans* bloodstream infections

Patient	Features of bloodstream infection (BSI) Duration of BSI*	Antifungal minimum inhibitory concentrations (MICs) against index strains	Antifungal treatment and outcome**	Positive blood cultures (BCs) for WGsing and strain nomenclature***
MN	Endovascular infection Duration of BSI: 13 days	AmB: 0.5 µg/mL CSP: 0.125 µg/mL FLU: 0.125 µg/mL POS: 0.015 µg/mL VOR: 0.015 µg/mL	CSP: days 2-6 CSP+FLU: days 6-7 AmB: days 8-14 FLU: day 15 - plan for lifelong Alive, on chronic suppressive FLU	Baseline (D0): M1 to M5 D13 BC: N1 to N5
AB	Central line associated BSI Duration of BSI: 3 days	AmB: 0.5 µg/mL CSP: 0.125 µg/mL FLU: 0.06 µg/mL POS: 0.015 µg/mL VOR: 0.015 µg/mL	CSP: days 3-4 FLU: days 5-7 Alive	Baseline (D0): A1 to A5 D3 BC: B1 to B5
G	Intra-abdominal and ocular candidiasis Duration of BSI: 1 day	AmB: 0.5 µg/mL CSP: 0.5 µg/mL FLU: 0.06 µg/mL POS: 0.015 µg/mL VOR: 0.015 µg/mL	CSP: day 4 FLU: days 4-15 Alive	Baseline (D0): G1-G10
QR	Endovascular infection Duration of BSI: 12 days	AmB: 0.5 µg/mL CSP: 0.35 µg/mL FLU: 0.06 µg/mL POS: 0.015 µg/mL VOR: 0.015 µg/mL	CSP: days 1-2, days 21-40 FLU: days 3-4, D40-death CAP+FLU: days 5-20 No BSI recurrence after day 12 Died from liver failure	Baseline (D0): Q1 to Q5 D12 BC: R1 to R5

*Duration of BSI is dated from baseline positive blood culture on day 0. Therefore, 2 days would signify a positive blood culture collected 48-72 hours after the baseline positive blood culture was collected. **Days of antifungal treatment are dated from positive baseline blood culture on day 0. ***In 3 patients (MN, AB, QR), baseline positive (i.e., time of diagnosis) and last positive blood cultures collected after the institution of antifungal treatment were included in whole genome sequencing studies. For 1 patient (G), only the baseline blood culture was included.

WGSing: whole genome sequencing; D: day(s); AmB: amphotericin B; CSP: caspofungin; FLU: fluconazole; POS: posaconazole; VOR: voriconazole

Supplemental Table 2. Within-patient genetic variations among *Candida albicans* strains from blood cultures.

Patient	BC bottle (time points)	Strains	SNPs					INDELs		Aneuploidy	LOH
			Total SNPs	Syn		Non-Syn					
				Het	Hom	Het	Hom	Het	Hom		
AB	Day 0	A1	7	3	1	2	1	0	0	-	
		A2	4	2	0	1	1	0	0	-	-
		A3	3	0	1	1	1	0	0	-	-
		A4	1	0	1	0	0	0	0	-	-
		A5	0	0	0	0	0	0	0	-	-
	Day 3	B1	3	2	0	0	1	0	0	-	-
		B2	2	0	1	0	1	0	0	-	-
		B3	4	2	0	1	1	0	0	-	-
		B4	0	0	0	0	0	0	0	-	-
		B5	3	1	1	0	1	0	0	-	-
G	Day 0	G1	42	5	9	10	18	7	1	trisomy Chr 5	-
		G2	19	4	3	7	5	2	1	-	-
		G3	13	3	2	4	4	3	0	-	-
		G4	15	3	3	7	2	3	0	-	-
		G5	7	1	2	2	2	1	1	-	-
		G6	28	3	6	7	12	1	0	-	-
		G7	20	3	4	7	6	6	2	-	-
		G8	30	3	5	9	13	5	1	-	-
		G9	11	1	3	3	4	1	2	-	-
		G10	15	4	1	7	3	5	0	-	-
MN	Day 0	M1	18	5	2	7	4	2	0	trisomy Chr 7	-
		M2	23	5	2	13	3	3	0	-	-
		M3	30	6	9	9	6	1	0	trisomy Chr 7	-
		M4	3	0	0	3	0	1	0	trisomy Chr 7	-

		M5	19	4	6	6	3	0	0	trisomy Chr 7	-
	Day 14	N1	13	3	2	3	5	0	0	-	-
		N2	36	6	6	18	6	7	2	-	-
		N3	3	0	0	3	0	0	0	-	-
		N4	29	4	8	11	6	2	0	-	-
		N5	18	2	2	12	2	4	0	-	-
QR	Day 0	Q1	24	1	5	7	11	4	0	-	Chr 1
		Q2	28	3	5	6	14	5	1	-	Chr 1
		Q3	19	8	2	9	0	4	0	-	
		Q4	23	2	5	5	11	1	0	-	
		Q5	24	2	5	5	12	2	1	-	
	Day 12	R1	10	2	1	5	2	2	0	-	Chr 1
		R2	8	3	0	5	0	1	0	-	Chr 1
		R3	18	1	4	3	10	2	0	-	Chr 1
		R4	12	3	1	5	3	2	3	-	Chr 1
		R5	18	1	4	3	10	1	0	-	Chr 1

SNPs and INDELs reported were defined as variants present in ≥ 1 strain but not all strains from a given patient, compared to reference strain SC5314

BC: blood culture; SNP: single nucleotide polymorphism; indel: insertion-deletion; LOH: loss of heterozygosity; syn: synonymous; non-syn: non-synonymous; het: heterozygous; hom: homozygous; chr: chromoso

Supplemental Table 3. Validation of Tri7 among *C. albicans* strains recovered from blood cultures of patient MN.

Blood culture	Strain	Biofilm (relative to strain M2)	CHR7-region 1		CHR7-region 2		CHR7-region 3	
			Mean	SEM	Mean	SEM	Mean	SEM
BC D0	M2S1	0.11	2.69	0.12	3.54	0.05	2.49	0.14
	M2S2	0.15	2.64	0.06	3.1	0.09	3.02	0.11
	M2S3	0.12	2.69	0.02	3.23	0.01	2.95	0.24
	M2S4	0.12	2.45	0.04	3.63	0.23	2.63	0.28
	M2S5	0.09	2.8	0.08	3.9	0.21	2.4	0.31
	M2S6	0.16	2.49	0.11	2.97	0.21	2.43	0.26
	M2S7	0.15	2.64	0.06	3.19	0.31	2.38	0.18
	M2S23	0.82	1.65	0.02	2.25	0.04	1.53	0.05
	M2S24	0.59	1.93	0.06	2.5	0.00	1.88	0.05
	M2S50	1.0	2.15	0.06	2.22	0.11	2.17	0.05
BC D13	M6S22	0.40	1.87	0.2	1.93	0.08	2.16	0.23
	M6S32	0.37	2.12	0.1	1.95	0.16	2.39	0.19
	M6S57	1.02	1.7	0.03	2.26	0.02	1.79	0.19
	M6S59	0.91	1.61	0.08	2.27	0.39	1.84	0.5
	M6S69	1.55	1.46	0.14	2.29	0.37	1.91	0.64
	M6S71	0.90	1.49	0.19	2.22	0.36	1.69	0.31
	M6S78	0.71	1.68	0.1	2.41	0.53	1.88	0.29
	M6S85	0.99	1.52	0.03	2.3	0.08	1.49	0.09
	M6S94	0.67	1.37	0.1	2.1	0.01	1.26	0.09
	M6S96	0.91	1.45	0.11	2.04	0.2	1.52	0.09
Control	M1	0.16	3.11	0.26	3.13	0.37	2.75	0.31
	M2	1.0	2	0	2	0	2	0
	M1	0.12	3	0.23	3.3	0.33	2.81	0.42
	M2	1.0	2	0	2	0	2	0

Biofilm formation by strains relative to euploid strain M2 is shown, as measured by OD_{590}. In screening strains, biofilm formation ≤ 30% was taken as a marker for Tri7. Ploidy of Chr7 was confirmed by qPCR of 3 regions from 10 strains from baseline (d0) and d13 blood cultures. There is a 100% correlation between Tri7 and relative biofilm at 30% cut-off.

Supplemental Table 4. Strains and plasmids used in this study

Strains	Source	Strain description	Reference
Patient AB			
A1	Initial blood culture, d0	Index strain, recovered by micro lab	This study
A2-A5	Initial blood culture, d0	Studied strains, recovered by PI lab	
B6	Subsequent blood culture, d12	Index strain, recovered by micro lab	
B7-10	Subsequent blood culture, d12	Studied strains, recovered by PI lab	
Patient G			
G1	Initial blood culture, d0	Index strain, recovered by micro lab	This study
G2-G10	Initial blood culture, d0	Studied strains, recovered by PI lab	
Patient MN			
M1	Initial blood culture, d0	Index strain, recovered by micro lab	This study
M2-M5	Initial blood culture, d0	Studied strains, recovered by PI lab	
N6	Subsequent blood culture, d13	Index strain, recovered by micro lab	

N7-10	Subsequent blood culture, d13	Studied strains, recovered by PI lab	
Patient QR			
Q1	Initial blood culture, d0	Index strain, recovered by micro lab	This study
Q2-Q5	Initial blood culture, d0	Studied strains, recovered by PI lab	
R6	Subsequent blood culture, d11	Index strain, recovered by micro lab	
R6-R10	Subsequent blood culture, d11	Studied strains, recovered by PI lab	
Other strains			
Barcoded-M1	From M1 strain	PI lab	This study
Barcoded-M2	From M2 strain	PI lab	
NRG1- overexpressed in M2	From M2 strain	PI lab	
Plasmids			
Plasmids RB793	For barcoding of M1	Addgene #199121	
Plasmid RB794	For barcoding of M2	Addgene #199122	
pCJN542	provided by Mitchell AP	*NRG1* over-expression	

Supplemental Table 5. Reagents and material used in this study

Medium	
Sabouraud dextrose agar	Fisher Scientific, DF0109-07-07-3
Yeast peptone dextrose (YPD)	Yeast Extract: BD Difco, 210929 Peptone: BD Difco, 11677 Dextrose: Fisher Scientific, D16-500
Spider medium	Nutrient broth: Fisher Scientific, DF0003-17-8 Mannitol: Fisher Sicentific, AC125345000 Potassium Phosphate Dibasic: Fisher Scientific, 7758-11-4 Agar, Fisher Scientific, DF0140-01-0
RPMI 1640 medium	Sigma Aldrich, R1383
Chemicals	
Crystal violet	Fisher Scientific, C581-100
DTT	Sigma Aldrich, 11583786001
EDTA	Sigma Aldrich, E8008
Glucose	Fisher Scientific, 50-99-7
Phosphate buffer saline	Fisher Scientific, R582350010F
Sorbitol	Fisher Scientific, BP439-500

Reagents/enzymes	
DNaseI	New England Biolabs, M0303L
Lyticase	Fisher Scientific, NC1644419
NgoMIV	New England Biolabs, R0564S
Antimicrobial agents	
Ampicillin	Fisher Scientific, BP1760-25
Chloramphenicol	Fisher Scientific, AC227921000
Kanamycin	Fisher Scientific, AC450810500
Nourseothricin	GoldBio, N-500-500
Streptomycin	MP Biomedicals, 219454180
Anidulafungin	MedChemExpress, HY13553
Fluconazole	Fisher Scientific 86386-73-4
Isavuconazole	BOC Sciences, 241479-67-4
Micafungin	MedChemExpress, HY-16321
Posaconazole	Fisher Scientific (TCI America products), P2477
Voriconazole	Fisher Scientific (TCI America products) VO116

Kits	
PCR clean-up system	Promega, A9281
Phusion High-Fidelity PCR mix with HF buffer	New England Biolabs, M0531S
Qiagen's DNeasy Blood and Tissue Kit	Qiagen (Hilden, Germany), 69504
qRT-PCR mix	Fisher Scientific, FERK0223
RiboPure RNA purification kit for yeast	Invitrogen, AM1924
SYBR Green qPCR Master Mix	Fisher Scientific, FERK0223
Verso cDNA synthesis kit	Fisher Scientific, AB1453A
Yeast DNA extraction kit	ThermoFisher, 788707
Zymobiomics DNA Miniprep kit	ZymoResearch, D4300
Others	
FBS (Fetal Bovine Serum)	HyClone, SH30071.02
Sterile culture bottle BD BACTEC Plus Aerobic medium	Fisher Scientific, BD442023

Supplemental Table 6. Primers used in this study

Name	Sequence (5'-3')	Experiments	Ref
4866 (NAT1 3' CHK F)	CAGATGCGAAGTTAAGTGCG	Strain barcoding	Kakade PMID: 36893271
4867 (Neut5 3' CHK R)	GGAGAGATCCATTAAGAGCAA	Strain barcoding	Kakade PMID: 36893271
4868 (Neut5 5' CHK F)	CTGAGATGGGGGATGTAAGTT	Strain barcoding	Kakade PMID: 36893271
4869 (NAT1 5' CHK R)	CAATAGCTTCAGCATCACCTG	Strain barcoding	Kakade PMID: 36893271
Chr1-F	GGACCAGCGATAGCCAATGA	Copy number determination	Kakade PMID: 36893271
Chr1-R	AGACCGCCAATCTTGTCTCA	Copy number determination	Kakade PMID: 36893271
Chr4-F	TGGTGTAGTTGGGGTTTCCA	Copy number determination	Kakade PMID: 36893271
Chr4-R	CCAAGGTGCCGTGACTTTTC	Copy number determination	Kakade PMID: 36893271
Chr7-F-1	CATTGGTGGTGGTGTTGGTG	Copy number determination	Kakade PMID: 36893271
Chr7-R-1	GCTAATGATCCACCAGAAATGGG	Copy number determination	Kakade PMID: 36893271
Chr7-F-2	ACTCACGATGCTGCAAAACG	Copy number determination	Kakade PMID: 36893271
Chr7-R-2	CCCCAGCAATAACTCCACCA	Copy number	Kakade

		determination	PMID: 36893271
Chr7-F-3	TTCCTGTTCGGGAGACACCT	Copy number determination	Kakade PMID: 36893271
Chr7-R-3	CCTGTTGGTGTTGAACGCAG	Copy number determination	Kakade PMID: 36893271
CalMIG1F	CCCAATGCTACTACAGCTACAA	Copy number determination	This study
CalMIG1R	AGCATAAGAACCAGGAGGTAAAT	Copy number determination	This study
CalMID1F	CCACCACCACCAACAATGATA	Copy number determination	This study
CalMID1R	TGTCCATTGTGCTGTACGATTAG	Copy number determination	This study
CalFAS1F	TGACTCCAACCACTGTCAATAC	Copy number determination	This study
CalFAS1R	GGTCATCATAACCGGTGAGAAA	Copy number determination	This study
NRG1-OE-F	TTTTCCTTGATTGTTGTTTGTTGCATTTT AGTTTTAGTTTTATTTTTTGAAGTCACAAA TTGTGAGCTTGGATC AAG CTT GCC TCG TCC CC	Over-expression of *NRG1*	This study
NRG1-OE-R	AGCAGCACTAGCATTTAATAACTTATTTG TTATTGGATATGATTGTTGATAAAGCATTG TTAATTA ATT TGA TTG TAA AGT TTG TTG ATG	Over-expression of *NRG1*	This study

CaEFB1-F	ATTGAACGAATTCTTGGCTGAC	Gene expression	Cheng PMID:12787355
CaEFB1-R	CATCTTCTTCAACAGCAGCTTG	Gene expression	Cheng PMID:12787355
Ca18S-F	TCTTTCTTGATTTTGTGGGTGG	Gene expression	CAO PMID: 18374543
Ca18S-R	TCGATAGTCCCTCTAAGAAGTG	Gene expression	CAO PMID: 18374543.
NRG1-F	CAC CTC ACT TGC AAC CCC	Gene expression	Uppuluri PMID: 20709787
NRG1-R	GCC CTG GAG ATG GTC TGA	Gene expression	PMID: 20709787
BC_For	AACAAAGAGAAAGCTCGGAGG	Bar code PCR	This study
BC_Rev	CGCAAATGATTATACATGGGG	Bar code PCR	This study

Bioinformatic analyses.

DNA was extracted using Qiagen's DNeasy Blood and Tissue Kit (Hilden, Germany).(Badrane, Cheng et al. 2023) DNA libraries were prepared with the Nextera XT (Illumina, San Diego) protocol and sequenced to ≥ 50X coverage with 2x150 bp paired end reads. Raw read zipped files were analyzed through a custom-built NextFlow pipeline, which integrates Burrows-Wheeler Aligner for reads mapping to the *C. albicans* SC5314 genome downloaded from Candida Genome Database (http://www.candidagenome.org/). The Genome Analysis Toolkit (GATK, v4.5.0.0) (McKenna, Hanna et al. 2010) was used for deduplicating and sorting of mapped reads, variant calling and filtering after a base quality score recalibration. SnpEff v4.5 was employed for variant annotation.(Cingolani, Platts et al. 2012) Low-confidence variants were filtered using GATK *VariantFiltration* tool. Variants were included if they fulfilled ≥ 1 of 4 stringent statistical criteria (i.e., variants were filtered if they failed all 4 criteria). The compound filtering expression was: Quality by Depth (QD) < 2; Fisher Strand (FS) > 60; mean square Mapping Quality (MQ) < 40. Additional filtering was applied through customized filtering criteria: minimum genotype quality (GQ) of 50; minimum of 80% support to the alternate allele in allele depth (AD), and minimum depth (DP) of 10. After filtration, the select variants tool extracted SNPs for final VCF files. VCF variant files from all strains were merged using BCFTOOLS.(Danecek, Bonfield et al. 2021) Whole genome multiple sequence alignment (MSA) was extracted from the multi-sample VCF file using VCF2MSA python script (https://github.com/tkchafin/vcf2msa.py). Fasta aligned sequences for each contig were extracted from the merged VCF file using a python script (https://github.com/Bahler-Lab/alignment-from-vcf). All aligned contigs were then merged and converted to a phylip format using a perl script (https://github.com/nylander/catfasta2phyml). A phylogenomic tree was built using RaxML(Kozlov, Darriba et al. 2019) and visualized in iTol v6.(Letunic and Bork 2021)

***In vitro* phenotypic assays.**

In vitro growth. *C. albicans* strains were grown in liquid YPD medium overnight at 30°C and diluted in YPD or RPMI1640 with 2% dextrose to OD_{600} (Optical Density, 600 nm) of 0.1. Diluted cultures were added to 96-well plates in triplicate with 200 µL per well, and growth was monitored at 30°C for 24h in a microplate reader (Molecular Device). Growth curves were analyzed using GraphPad Prism 9. Experiments were performed with 3 biological replicates.

In vitro filamentation. Strains were grown overnight in liquid YPD at 30°C and then cultured in YPD, YPD containing 10% Fetal Bovine Serum (FBS), RPMI1640 with 2% glucose or Spider media at 37 °C for 4 h with shaking (200 rpm). Cell suspensions were removed hourly and imaged using microscopy. For filamentation on solid medium, overnight culture grown in YPD at 30ºC was washed and adjusted to 10^7 cells/mL in normal saline; 5 µl were spotted on agar plate and incubated at 30ºC.

Antifungal susceptibility testing and tolerance assays. The sensitivity to cell wall stress-inducing agents were assessed by spotting 5 µL of serial ten-fold dilutions of each strain grown overnight in YPD onto SDA plates impregnated with the indicated chemical agent. The plates were incubated at 30 and 40°C until colonies appeared. Antifungal susceptibility testing was performed using the broth dilution technique according to the Clinical and Laboratory Standards Institute (CLSI) standardized method.((CLSI)) Concentrations ranged from 0.25-256 µg/mL for fluconazole (Fisher Scientific 86386-73-4), and 0.015-16 µg/mL for echinocandins. At 24 hours, the wells were read visually with a viewing mirror. MIC was set at the lowest drug concentration at which there was a ≥ 50% decrease in growth, relative to growth in no drug containing wells. The plates were also were read using a spectrophotometer reader (SPECTROstar, BMG labtech)) at OD600nm for determination of tolerance. Supra-MIC growth (SMG) was calculated as the average growth per well above the MIC divided by the level of growth without drug.(Rosenberg, Ene et al. 2018, Berman and Krysan 2020) Tolerance was also quantified using disk diffusion.(Rosenberg, Ene et al. 2018, Berman and Krysan 2020) For disk diffusion, overnight growth *C. albicans* cells (2×10^5 CFU) were spread onto casitone plates (9 g/l

Bacto casitone, 5 g/l yeast extract, 15 g/l Bacto agar, 11.5 g/l sodium citrate dehydrate and 2% glucose) with a cotton swab and allowed to air dry for ~30 min. A filter disk containing micafungin (5ug) was placed in the center of the plate and allowed to grow at 35°C for 48 hours. The radius corresponding to the point where growth was inhibited by 20%, 50% or 80% relative to the maximum radius, was measured. Tolerance levels were determined from the degree of growth within the region of growth inhibition detected visually on the plates and calculated using *diskImageR* and imageJ (fraction of growth, FoG_{20}, FoG_{50}, FoG_{80}, respectively).

Biofilm formation.

Biofilms were formed in flat-bottomed 96-well microplates. For each strain, a cell suspension in normal saline was adjusted to McFarland 0.5 and 1:10 diluted in RPMI1640 medium supplemented with 2% (w/v) glucose. Plate wells were inoculated with 200 µL of standardized *C.albicans* suspension in triplicate and incubated at 37 °C for 90 minutes to allow cell adhesion. A negative control was prepared by inoculating 200 µL RPMI1640 medium. After the adhesion phase, non-adherent cells were removed by thoroughly washing the wells with 0.15 M sterile phosphate-buffered saline (PBS, pH 7.2). Each well was then filled with 200 µL of fresh RPMI1640 medium, and plates were incubated at 37°C for 24h to allow biofilm formation. To assess biofilm formation, culture broth was gently aspirated, and each well was washed twice with PBS and incubated with 100 µL methanol for 15 min at room temperature. Plates were left to dry completely in a chemical safety cabinet, followed by staining with 100 µL 0.1% crystal violet for 5 min and three washes with dH_2O. Crystal violet was dissolved from the stained biomass by adding 100 µL of 33% acetic acid and by plate shaking for 1 min at 800 rpm. Supernatants of dissolved crystal violet were transferred into fresh wells of a 96-well plate, and absorbance at 590 nm was recorded using a micro plate reader (Molecular Device).

(CLSI), C. a. L. S. I. "Reference Method for Broth Dilution Antifungal Susceptibility Testing of Yeasts. 4th ed. CLSI standard M27. Wayne, PA: Clinical and Laboratory Standards Institute; 2017."

Badrane, H., S. Cheng, C. L. Dupont, B. Hao, E. Driscoll, K. Morder, G. Liu, A. Newbrough, G. Fleres, D. Kaul, J. L. Espinoza, C. J. Clancy and M. H. Nguyen (2023). "Genotypic diversity and unrecognized antifungal resistance among populations of Candida glabrata from positive blood cultures." Res Sq.
Berman, J. and D. J. Krysan (2020). "Drug resistance and tolerance in fungi." Nat Rev Microbiol **18**(6): 319-331.
Cingolani, P., A. Platts, L. L. Wang, M. Coon, T. Nguyen, L. Wang, S. J. Land, X. Lu and D. M. Ruden (2012). "A program for annotating and predicting the effects of single nucleotide polymorphisms, SnpEff." Fly **6**(2): 80-92.
Danecek, P., J. K. Bonfield, J. Liddle, J. Marshall, V. Ohan, M. O. Pollard, A. Whitwham, T. Keane, S. A. McCarthy, R. M. Davies and H. Li (2021). "Twelve years of SAMtools and BCFtools." GigaScience **10**(2).
Kozlov, A. M., D. Darriba, T. Flouri, B. Morel and A. Stamatakis (2019). "RAxML-NG: a fast, scalable and user-friendly tool for maximum likelihood phylogenetic inference." Bioinformatics **35**(21): 4453-4455.
Letunic, I. and P. Bork (2021). "Interactive Tree Of Life (iTOL) v5: an online tool for phylogenetic tree display and annotation." Nucleic Acids Research **49**(W1): W293-W296.
McKenna, A., M. Hanna, E. Banks, A. Sivachenko, K. Cibulskis, A. Kernytsky, K. Garimella, D. Altshuler, S. Gabriel, M. Daly and M. A. Depristo (2010). "The Genome Analysis Toolkit: A MapReduce framework for analyzing next-generation DNA sequencing data." Genome Research **20**(9): 1297-1303.
Rosenberg, A., I. V. Ene, M. Bibi, S. Zakin, E. S. Segal, N. Ziv, A. M. Dahan, A. L. Colombo, R. J. Bennett and J. Berman (2018). "Antifungal tolerance is a subpopulation effect distinct from resistance and is associated with persistent candidemia." Nat Commun **9**(1): 2470.